UNIVERSIDAD DE INVESTIGACIÓN DE TECNOLOGÍA EXPERIMENTAL YACHAY

Escuela de Ciencias Biológicas e Ingeniería

TÍTULO: Synthesis and characterization of cellulose-based hydrogels for antibiotic delivery against Leishmaniasis

Trabajo de integración curricular presentado como requisito para la obtención del título de Ingeniería Biomédica

Autor:

Andrea Carolina Serrano Larrea

Tutor:

Ph.D. Frank Alexis

Co-tutor:

MSC. Javier Santamaría

Urcuquí, enero de 2020

Urcuquí, 12 de febrero de 2020

SECRETARÍA GENERAL
(Vicerrectorado Académico/Cancillería)
ESCUELA DE CIENCIAS BIOLÓGICAS E INGENIERÍA
CARRERA DE BIOMEDICINA
ACTA DE DEFENSA No. UITEY-BIO-2020-00003-AD

En la ciudad de San Miguel de Urcuquí, Provincia de Imbabura, a los 12 días del mes de febrero de 2020, a las 11:30 horas, en el Aula CHA-01 de la Universidad de Investigación de Tecnología Experimental Yachay y ante el Tribunal Calificador, integrado por los docentes:

Presidente Tribunal de Defensa	Dr. SANTIAGO VISPO, NELSON FRANCISCO , Ph.D.
Miembro No Tutor	LIRA VERGARA RENE CONSTANZA
Tutor	Dr. ALEXIS FRANK , Ph.D.

Se presenta el(la) señor(ita) estudiante **SERRANO LARREA, ANDREA CAROLINA**, con cédula de identidad No. **0105125199**, de la **ESCUELA DE CIENCIAS BIOLÓGICAS E INGENIERÍA**, de la Carrera de **BIOMEDICINA**, aprobada por el Consejo de Educación Superior (CES), mediante Resolución **RPC-SO-43-No.496-2014**, con el objeto de rendir la sustentación de su trabajo de titulación denominado: **SYNTHESIS AND CHARACTERIZATION OF CELLULOSE-BASED HYDROGELS FOR ANTIBIOTIC DELIVERY AGAINST LEISHMANIASIS**, previa a la obtención del título de **INGENIERO/A BIOMÉDICO/A**.

El citado trabajo de titulación, fue debidamente aprobado por el(los) docente(s):

Tutor	Dr. ALEXIS FRANK , Ph.D.

Y recibió las observaciones de los otros miembros del Tribunal Calificador, las mismas que han sido incorporadas por el(la) estudiante.

Previamente cumplidos los requisitos legales y reglamentarios, el trabajo de titulación fue sustentado por el(la) estudiante y examinado por los miembros del Tribunal Calificador. Escuchada la sustentación del trabajo de titulación, que integró la exposición de el(la) estudiante sobre el contenido de la misma y las preguntas formuladas por los miembros del Tribunal, se califica la sustentación del trabajo de titulación con las siguientes calificaciones:

Tipo	Docente	Calificación
Miembro Tribunal De Defensa	LIRA VERGARA RENE CONSTANZA	9.9
Presidente Tribunal De Defensa	Dr. SANTIAGO VISPO, NELSON FRANCISCO , Ph.D.	10.0
Tutor	Dr. ALEXIS FRANK , Ph.D.	10.0

Lo que da un promedio de: **10 (Diez punto Cero)**, sobre 10 (diez), equivalente a: **APROBADO**

Para constancia de lo actuado, firman los miembros del Tribunal Calificador, el/la estudiante y el/la secretario ad-hoc.

SERRANO LARREA, ANDREA CAROLINA
Estudiante

Dr. SANTIAGO VISPO, NELSON FRANCISCO , Ph.D.
Presidente Tribunal de Defensa

Dr. ALEXIS FRANK , Ph.D.
Tutor

LIRA VERGARA RENE CONSTANZA
Miembro No Tutor

ALARCON FELIX, KARLA ESTFANIA
Secretario Ad-hoc

AUTORÍA

Yo, **ANDREA CAROLINA SERRANO LARREA**, con cédula de identidad 0105125199, declaro que las ideas, juicios, valoraciones, interpretaciones, consultas bibliográficas, definiciones y conceptualizaciones expuestas en el presente trabajo; así cómo, los procedimientos y herramientas utilizadas en la investigación, son de absoluta responsabilidad de el/la autora (a) del trabajo de integración curricular. Así mismo, me acojo a los reglamentos internos de la Universidad de Investigación de Tecnología Experimental Yachay.

Urcuquí, enero 2020

Andrea Carolina Serrano Larrea
CI: 0105125199

AUTORIZACIÓN DE PUBLICACIÓN

Yo, **ANDREA CAROLINA SERRANO LARREA**, con cédula de identidad 0105125199, cedo a la Universidad de Tecnología Experimental Yachay, los derechos de publicación de la presente obra, sin que deba haber un reconocimiento económico por este concepto. Declaro además que el texto del presente trabajo de titulación no podrá ser cedido a ninguna empresa editorial para su publicación u otros fines, sin contar previamente con la autorización escrita de la Universidad.

Asimismo, autorizo a la Universidad que realice la digitalización y publicación de este trabajo de integración curricular en el repositorio virtual, de conformidad a lo dispuesto en el Art. 144 de la Ley Orgánica de Educación Superior

Urcuquí, enero 2020

Andrea Carolina Serrano Larrea
CI: 0105125199

Dedicatoria

Dedico este trabajo a mis padres Imelda y Leonardo, gracias a su amor, trabajo y dedicación me han ayudado a cumplir una meta más en mi vida.

A mi hermana Dani que siempre ha estado apoyándome en cada paso dado.

A mis abuelos Papi Coqui y Mami Rebe que siempre han estado a mi lado en cada logro y caída apoyándome.

A las grandes amistades de la universidad.

A mis compañeras de laboratorio que siempre estuvieron apoyándome y enseñándome.

A mis profesores de la Escuela de Ciencias Biológicas e Ingeniería

Andrea Carolina Serrano Larrea

Agradecimientos

Quiero agradecer a mi familia por siempre ser un soporte incondicional en cada decisión tomada. A mis padres por su apoyo y sacrificio para que nunca me falte nada durante mi carrera universitaria. A mi hermana por ayudarme en todo mi trabajo y ser un apoyo fundamental. A mi abuelo papi Coqui por siempre estar presente en cada uno de los pasos dados en mi carrera.

Agradezco a mi tutor Dr. Frank Alexis por ser un gran mentor y brindarme siempre su apoyo durante esta investigación.

A mi cotutor Javier Santamaría por su ayuda, guía y sabios consejos.

A Eliana Lara por ser una su apoyo incondicional como amiga y tutora, a Gabriela Morales, Pamela Mosquera y Jessenia Basantes por ser las mejores compañeras de laboratorio y grandes amigas.

Al Instituto de Investigación en Salud Pública y Zoonosis-CIZ por permitirme realizar parte de este proyecto en sus instalaciones.

Finalmente, agradezco a la Universidad Yachay Tech y a todos los profesores de la Escuela de Ciencias Biológicas e Ingeniería, especialmente a Nelson, Reneé, Si Amar, Graciela, Roberto, Ming Ni, quienes han sido parte de mi formación como Ingeniera Biomédica.

Andrea Carolina Serrano Larrea

Resumen

La leishmaniasis es una enfermedad desatendida causada por protozoos del género Leishmania y presenta tres formas principales, leishmaniasis visceral, cutánea y mucocutánea. La leishmaniasis cutánea es un problema de salud pública en Ecuador debido a su amplia distribución, principalmente en las zonas rurales de las regiones de la Costa, Sierra y la Amazonía, se puede encontrar en 23 de las 24 provincias. El tratamiento de primera línea es antimoniato de meglumina,este presenta una gran cantidad de efectos adversos en el paciente, e incluso puede causar la muerte. Además, el costo del tratamiento es alto y está desarrollando resistencia. Debido a esto, se están buscando nuevas alternativas, como las fluoroquinolonas, las cuales se ha reportado que son activas en las topoisomerasas II de *Leishmania spp.*, además tiene menor costo y menos efectos adversos. Por otro lado, los hidrogeles basados en polímeros de polisacáridos naturales, como la celulosa, son de gran interés en aplicaciones biomédicas, más específicamente, para la regeneración de tejidos y la administración de fármacos. El objetivo de este trabajo es desarrollar hidrogeles a base de celulosa cargados con enrofloxacina para que tengan actividad antileishmanial contra los promastigotes de *Leishmania mexicana*. Los hidrogeles se preparan utilizando métodos de disolución con la carga del antibiótico durante el proceso de fabricación para evitar la pérdida del compuesto activo. El perfil de liberación y la permeabilidad transdérmica se estudiaron utilizando la celda de difusión de Franz. Finalmente, estos hidrogeles han presentado excelentes resultados en el proceso de liberación de antibióticos en pH ácido para ser usado en heridas cutáneas de leishmaniasis, además, presentan un alto nivel de actividad antileishmanial. Los datos obtenidos promueven el uso de estos hidrogeles para la curación de heridas por leishmaniasis cutánea.

Palabras clave:

Hidrogeles, Administración de fármacos, *Leishmania mexicana*, Leishmaniasis Cutánea, Celda de Franz

Abstract

Leishmaniasis is a neglected disease caused by protozoa of the genus *Leishmania*. It presents three main forms, visceral, cutaneous and mucocutaneous leishmaniasis. Cutaneous leishmaniasis is a public health problem in Ecuador because of its wide distribution, mainly in rural areas in the regions of Coast, Highlands, and Amazon. It can be found in 23 out of the 24 provinces. The first-line treatment is antimonate meglumine, and it has a large number of adverse effects in the patient and it can cause death. In addition, the cost of treatment is high, and it is developing resistance. Due to this, new alternatives are being sought, such as fluoroquinolones, which have been reported active on topoisomerases II of *Leishmania spp.*; it has lower cost and fewer adverse effects. On the other hand, hydrogels based on natural polysaccharide polymers, such as cellulose, are of great interest in biomedical applications, more specifically, for tissue regeneration and drug delivery. The aim of this work is to develop cellulose-based hydrogels that are loaded with enrofloxacin to have anti-leishmanial activity against promastigotes of *Leishmania mexicana*. Hydrogels are prepared using dissolving methods with the load of the antibiotic during the manufacturing process to avoid the loss of the active compound. The release profile and transdermal permeability were studied using the diffusion Franz Cell. Finally, these hydrogels have presented great results in the antibiotic release process in acid pH to be used in cutaneous wounds of Leishmaniasis. In addition, they present a high level of anti-leishmanial activity. The obtained data encouraged the use of these hydrogels for cutaneous leishmaniasis wound healing.

Key-words:

Hydrogels, Cellulose, Drug Delivery, *Leishmania mexicana*, Cutaneous Leishmaniasis, Franz Cell

INDEX

List of Figures

List of Schemes

List of Tables

List of Equations

List of Annex

1. INTRODUCTION – JUSTIFICATION

1.1 Leishmaniasis

Leishmaniasis is a parasitoid disease produced by protozoa of the genus *Leishmania*, of intracellular location, transmitted by the bite of Diptera insects of the family *Phlebotomidae*, genera *Phlebotomus* and *Lutzomyia*. It presents three primary forms: visceral (VL), cutaneous (CL), and mucocutaneous leishmaniasis (MCL). This disease affects the most impoverished populations on the planet, and it is associated with malnutrition, population displacements, poor housing conditions, weak immune system and lack of resources, for this reasons, leishmaniasis is considered a neglected disease. Each year there are around 700,000 and one million new cases and between 26,000 and 65,000 deaths. (World of Health Organization, 2019)

Leishmania has two primary stages in its cycle: promastigote and amastigote. Promastigote is the extracellular stage that develops in the invertebrate vector. The amastigote is the intracellular stage in the bloodstream of a vertebrate host. The complete *Leishmania* cycle is presented in the figure below: (Uzcanga et al., 2017)

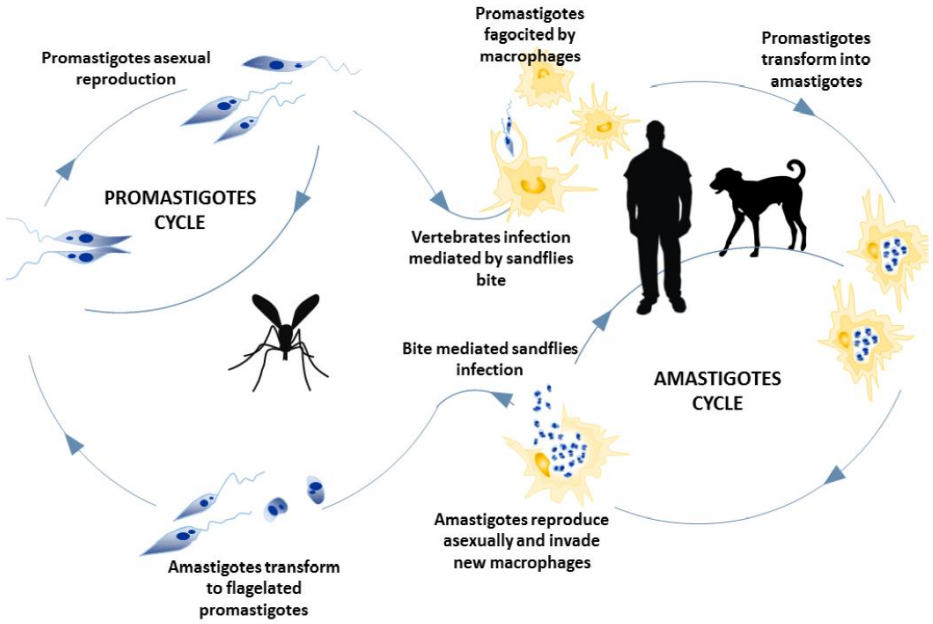

Figure 1: Lifecycle of Leishmania spp. (Uzcanga et al., 2017)

According to the WHO, CL is the most common form of leishmaniasis, and it produces ulcers and scars in the exposed areas of the body. CL is considered the less aggressive form of leishmaniasis. Old World leishmaniasis is endemic in the Eastern Hemisphere: Asia, Africa, and southern Europe. On the other hand, New World

leishmaniasis is endemic to the Western Hemisphere, mainly in Central and South America, except in Chile and Uruguay. (World of Health Organization, 2019)

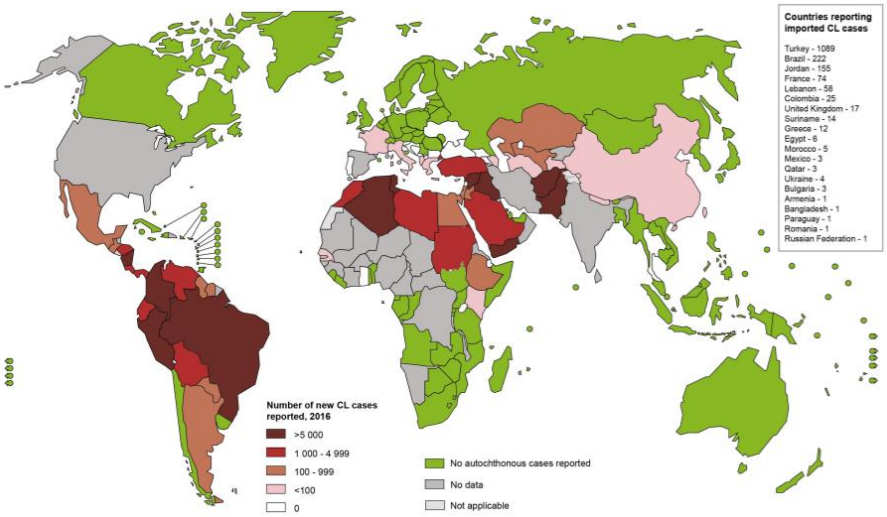

Figure 2: Status of endemicity of cutaneous leishmaniasis worldwide (World of Health Organization, 2016)

Figure 3: Geographical distribution of cutaneous and mucocutaneous leishmaniasis in the New World. Blue: Mucocutaneous; Yellow: Cutaneous Leishmaniasis (World of Health Organization, 2010)

In Ecuador, CL is considered a public health problem, and it is found in all the continental Ecuador. In this country, there are reports only for cases of CL and MCL. Parasite species found in Ecuador are *L. (V.) braziliensis, L. (V.) panamensis, L. (V.)*

guyanensis, L. (V.) naiffi, L. (L.) amazonensis, L. (V.) lainsoni, L. (L.) major-like, and *L. (L.) mexicana*. Vectors species prevalent are *Lu. trapidoi, Lu. hartmanni, Lu. gomezi, Lu. tortura, Lu. ayacuchensis*, and *Lu. maranonensis*. (Carrillo & Miranda, 2018; Hashiguchi et al., 2017)

Between 2001 and 2016, a total of 23,947 CL cases have been reported with an annual average of at least 1,500 cases. (Ministerio de Salud Pública del Ecuador, 2019). According to the WHO status of endemicity of CL, in 2017, 1632 new cases of endemic CL were reported. On the other hand, no autochthonous cases of VL were reported. Besides, the Public Health Minister reported 1051 cases of CL and 22 cases of MCL in 2018. (Ministerio de Salud Pública del Ecuador, 2019; World of Health Organization, 2018)

Figure 4: An 18-year-old male patient in Pichincha province has a 5 cm leishmaniasis ulcer in his neck (Carrillo & Miranda, 2018)

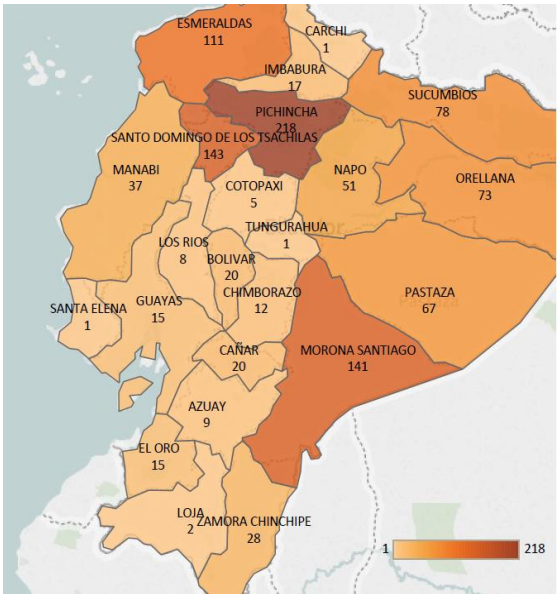

Figure 5: Cases of Leishmaniasis in Ecuador, 2018. (MSP, 2019)

1.2 Fluoroquinolones

Fluoroquinolones are synthetic analogs of nalidixic acid, have a fluorine atom attached to the quinolone ring at position C-6, which presents activity against gram-negative and gram-positive bacteria (Leyva & Leyva, 2008). Fluoroquinolones inhibit DNA topoisomerase II and topoisomerase IV, which are involved in the transcription, recombination, replication, and repair of the DNA, thus, leading to cell death (Otero, Mestorino, & Errecalde, 2000).

The work carried out by Esteves & Santamaría (2018) determined the anti-leishmanial activity of fluoroquinolones: enrofloxacin, levofloxacin, ciprofloxacin, and moxifloxacin. This anti-leishmanial activity was compared with meglumine antimoniate for promastigotes of *L. mexicana* and *L. braziliensis*. Their results indicated that enrofloxacin showed higher activity than the other fluoroquinolones tested; the four fluoroquinolones have a lower minimal inhibitory concentration (MIC), non-inhibitory concentration (NIC), and half-maximal inhibitory concentration (IC50) than meglumine antimonite, which is the current treatment of leishmaniasis. (Esteves & Santamaría, 2018)

Table 1: Values of MIC, NIC, IC50 of fluoroquinolones in Leishmania Mexicana described by Esteves & Santamaría, 2018

	MIC (uM)	**NIC (uM)**	**IC50 (uM)**	**R^2**
Enrofloxacin	7216	234.9	1498	0.9974
Levofloxacin	21481	384.5	4718	0.9888
Ciprofloxacin	27517	2099	8582	0.9785
Moxifloxacin	205212	9464	50282	0.9933
Meglumine antimonite	470235	176898	302360	0.9712

1.2.1 Enrofloxacin

Enrofloxacin has a role as an antibacterial agent, an antineoplastic agent, and an antimicrobial agent of veterinary use. Its molecular weight is 359,39 g/mol (National Center for Biotechnology Information, n.d.)

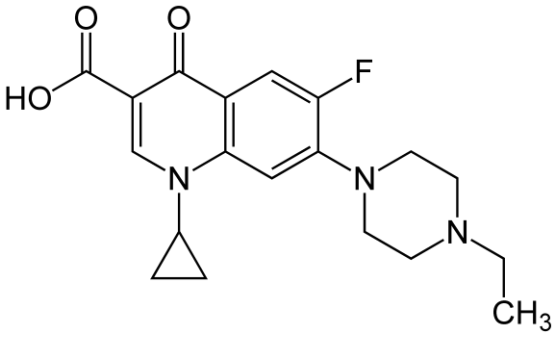

Figure 6: Chemical structure of enrofloxacin. (National Center for Biotechnology Information, n.d.)

Depending on the pH, enrofloxacin can exist in four possible forms:

a) Neutral pH: Non-ionized form (N)
b) Acid pH: Cationic form (C)
c) Basic pH: Anionic form (A)
d) Neutral pH: Zwitterion form (Z)

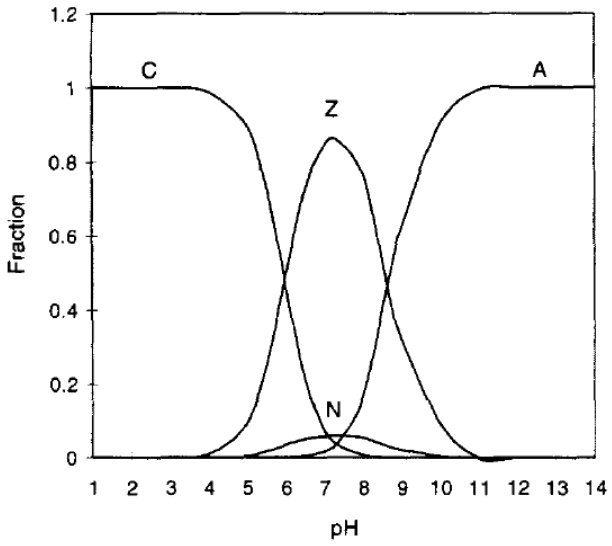

Figure 7: Distribution of the molar fraction of the four forms: A, C, N, Z. (Lizondo, Pons, Gallardo, & Estelrich, 1997)

The aqueous solubility of enrofloxacin is explained by its ionization.

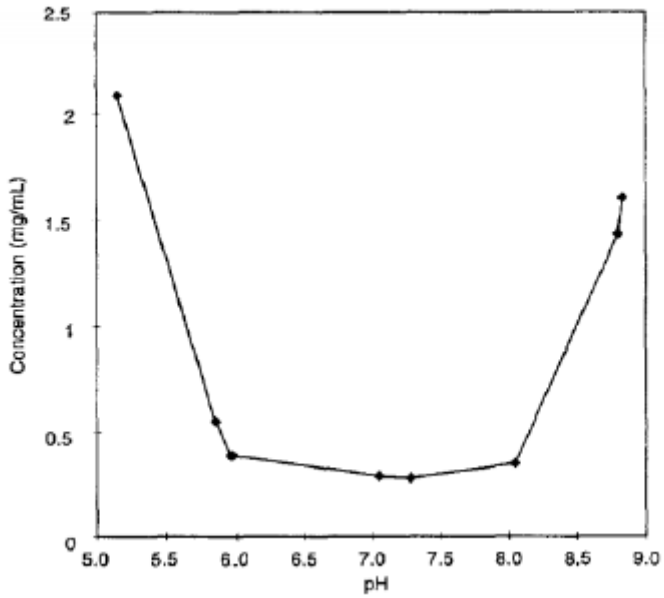

Figure 8: Solubility/pH profile of enrofloxacin. (Lizondo et al., 1997)

The maximum aqueous solubility is at pH 5.02, where the cationic and the zwitterion form predominate. On the other hand, enrofloxacin presents a low aqueous solubility near the isoelectric point, where the zwitterion form predominates, but a high lipid solubility, which facilitates its diffusion within biological tissues, including bacterial cells. Finally, at a basic pH, high than 8.5 enrofloxacin presents a high solubility in the anionic form. (Lizondo et al., 1997)

1.3 Cellulose-based Hydrogels

Cellulose $(C_6H_{12}O_6)_n$ is the most abundant biopolymer on the earth and presents excellent properties such as no taste, odorless, hydrophilic, biodegradable, and biocompatible (Heinze, 2015). Hydrogels are defined as two- or multi-component systems consisting of a 3D network of polymer chains and water that fills the space between macromolecules. Depending on the polymer and the physical and chemical properties of the hydrogel, it could have different applications (Ahmed, 2015). Nowadays, cellulose-based hydrogels have gained particular attention in the biomedical field. *Figure 9* illustrates the different applications of cellulose-based hydrogels.

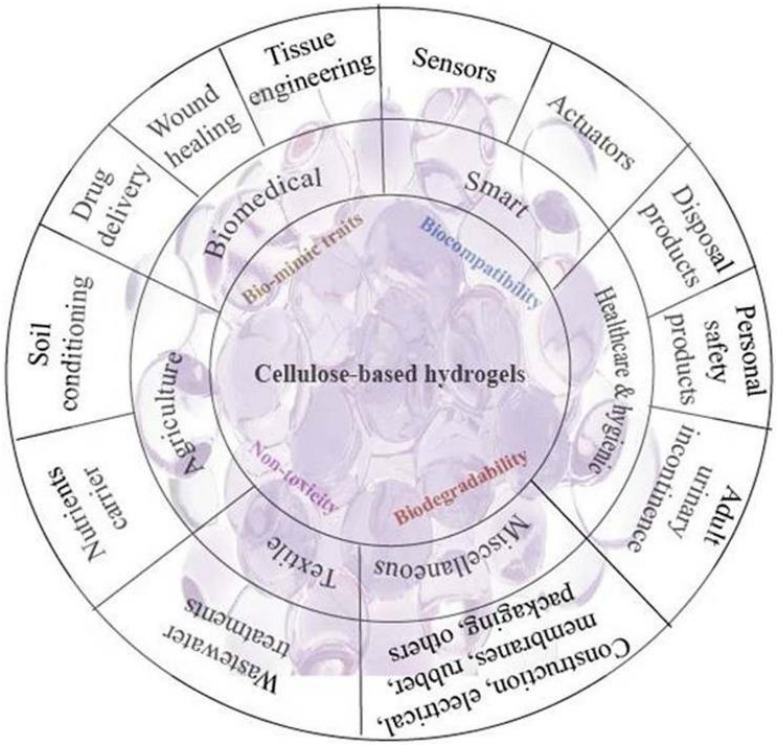

Figure 9: Different applications of cellulose-based hydrogels in the biomedical field. (Kabir et al., 2018)

Drug delivery is a new approach based on formulations, technologies, medical devices, and systems to transport molecules through the body and safely achieve its desired therapeutic effect at the target site. Moreover, localized drug delivery allows an easy self-administration for patients. (Zhang, Chang, & Leong. 2013). Drug release system using hydrogels function by the delivery of drugs at desired locations (tissue, cells) in response to different stimuli such as enzymes, pH, light, temperature, chemicals, electric fields, and magnetic fields. (Kabir et al., 2018)

1.4 Transdermal Drug Delivery (TDD)

TDD is a promising tool and provides several advantages over other methods of administration, such as ease of access, large surface area, reduced side effect, bypassing enzyme action, controlled release, among others. (Zakharova, Pashirova, Kashapov, Gabdrakhmanov, & Sinyashin, 2017)

A transdermal hydrogel is a medicated adhesive hydrogel that is placed on the skin to deliver medication through the skin and into the systemic circulation. TDD aims to deliver drugs into the bloodstream through the skin at a predetermined rate. (Himanshi Tanwar and Ruchika Sachdeva, 2016)

The skin is the largest organ of the body with a surface area approximated of $2m^2$. The skin prevents the entrance of various chemical and biological agents into the body, acting as a physiological barrier. The body temperature is around 37°C, while skin presents a temperature of around 32,5°C to 33,5°C and a pH between 4,7 and 5,75. Skin is one of the most readily available organs of the body. (Eucerin, n.d.; Himanshi Tanwar and Ruchika Sachdeva, 2016)

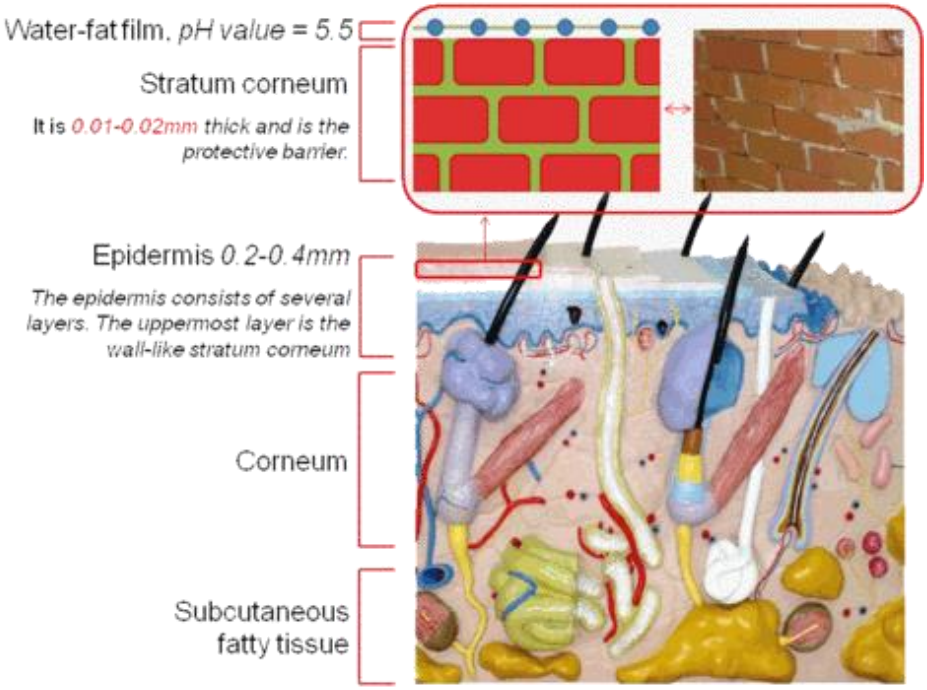

Figure 10: Skin barriers (SafeHair, n.d.)

The first barrier to overcome is the stratum corneum there are three main pathways to penetrate this barrier.

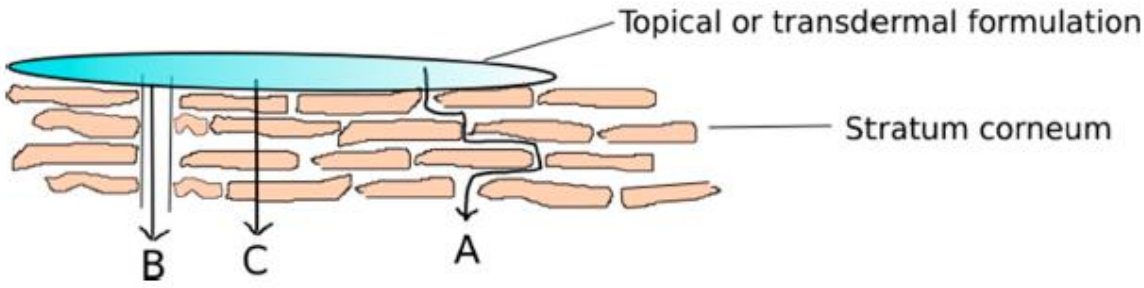

Figure 11: Penetration pathways for stratum corneum: A: intercellular, B: Follicular, C: Transcellular (Zsikó et al., 2019)

1.4.1 Franz Cell

Several diffusion cells have been described to determine in vitro permeability, among one of the most famous is the Franz cells. A useful way to analyze skin permeability is first to study how the molecules pass through inert (artificial) membranes and then use the skin model. Several studies have been published to study the diffusion of different medications through a synthetic or natural membrane that mimics the skin. (Aulton, 2004; Lasso & Ruiz, 2017; Llanga, 2019)

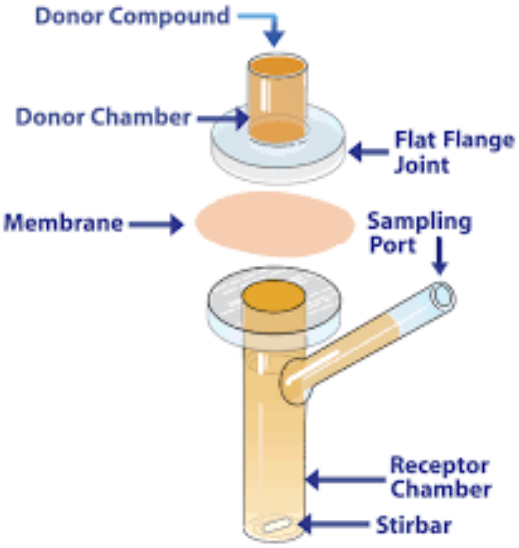

Figure 12: A typical model of a vertical diffusion Franz Cell system (Perm Gear, n.d.)

The diffusion Franz Cell is a mechanism consisting of two chambers, a donor and a recipient, separated by a membrane (animal, human or synthetic origin) that allows the diffusion of molecules from one chamber to another. In the donor compartment, a solution or dispersion containing the active compound is added. In the recipient compartment, the corresponding samples are taken, which are subsequently quantified by analytical techniques such as UV-vis spectrophotometer, chromatography, among others. These types of cells have been used frequently in the determination of the percutaneous absorption, drug release kinetics, and skin penetrability. (Estevez, Aguilera, Saez, & Hardy, 2000; Lasso & Ruiz, 2017; Llanga, 2019; Perm Gear, n.d.)

Diffusion is a spontaneous random movement of particles through a membrane or space due to a concentration gradient. The diffusion coefficient (D) is determined using Fick's laws of diffusion. (Dickson, 2019)

$$J = -D\frac{dC}{dt}$$

Equation 1: Fick's first law of diffusion

Where

J: Flux

D: Diffusion coefficient

C: Concentration gradient

t: time

With this equation, the diffusion coefficient can be determined if the flux and the change in the concentration over time are known. (Dickson, 2019)

Fick's second law of diffusion

This law describes the time course of the transfer of a solute between two reservoirs separated by a membrane. (Bruschi, 2015)

$$\frac{dC}{dt} = -D\frac{d^2C}{dx^2}$$

Equation 2: Fick's second law of diffusion

If we measure the accumulated mass of diffuser, m, which passes per unit area through the membrane as a function of time, we obtain the following equation:

$$\frac{dm}{dt} = \frac{DC_oK}{h}$$

Equation 3: Stable Flux

Where

dm/dt: stable flux

C_o: drug concentration in the donor solution

K: partition coefficient

h: membrane thickness

Most of the time is difficult to separate the diffusion coefficient (D) from the partition coefficient (K) in the biological membranes. It can be assumed that the permeability coefficient (P) is a composed parameter KD or KD/h (when h is uncertain, such as the skin), and know the permeability coefficient is known as Kp (Aulton, 2004)

1.5 Mathematical models for the release kinetics

There are several mathematical models that describe the release kinetics of a matrix loaded with an active substance. The most common release kinetic models are zero-order release kinetics, first-order release kinetics, Higuchi model, Hixson–Crowell model, and Korsmeyer–Peppas model. (Bruschi, 2015)

Table 2: Most common mathematical models used to describe drug release mechanism

(Baishya, 2017; Bruschi, 2015; Shaikh, Kshirgagar, & Patil, 2015)

Model	Mathematical Equation	Release Mechanism
Zero Order	$\boldsymbol{C = C_o - K_o t}$ *C*: Amount of drug released C_o: Initial amount of drug in solution (it is usually zero) K_o: Zero-order rate constant *t*: time	Diffusion
First Order	$\boldsymbol{LogC = LogC_o - Kt/2.303}$ C_o: Initial concentration of drug *K*: First order constant *t*: time	Fick's first law, diffusion
Higuchi Model	$\boldsymbol{C = [D(2qt - C_s)C_s t]^{1/2}}$ *C*: Total amount of drug released per unit area of the matrix *D*: Diffusion coefficient for the drug in the matrix *qt*: Total amount of drug in a unit volume of matrix C_s: Dimensional solubility of the drug in the polymer matrix *t*: Time	Diffusion medium based in Fick's first law mechanism
Hixson–Crowell Model	$\boldsymbol{{C_o}^{1/3} - {C_t}^{\frac{1}{3}} = K_{HC} t}$ C_t: Amount of drug released in time C_0: Initial amount of drug in the tablet. K_{HC}: Rate constant for the Hixson-Crowell equation.	Erosion release mechanism
Korsmeyer-Peppas Model	$F = \left(\frac{M_t}{M}\right) = K_m t^n$ F: Fraction of drug released at time "t" M_t: Amount of drug released at time "t" *M*: Total amount of drug in dosage form K_m: Kinetic constant *n*: diffusion or release exponent *t*:time	Semi empirical model, diffusion based mechanism

2. PROBLEM STATEMENT

2.1 Current treatment of leishmaniasis

The first-line treatment against Leishmaniasis is meglumine antimoniate (pentavalent antimonials); it presents a large number of adverse effects including nephrotoxicity, hepatoxicity, anorexia, headache, problems in the musculoskeletal system and can cause death. This therapy cannot be used in children or in old people; in addition, the cost of treatment is high, and it is developing resistance (World of Health Organization, 2019). According to Hashiguchi and collaborators (2017), in their review of Leishmaniasis in Ecuador, patients with CL are used to cut off the first-line treatment for an extended period due to the painfulness of the drug-injection, remoteness from their dwellings to health centers, and the adverse and toxic effects of the drug. As a result, resurgence or recurrence of CL cases after "clinical cure" but not "parasitological cure" of the treated-lesions, having an incomplete/immature regimens (discontinuance of treatment course) of the injection with the meglumine antimoniate. (Hashiguchi et al., 2017)

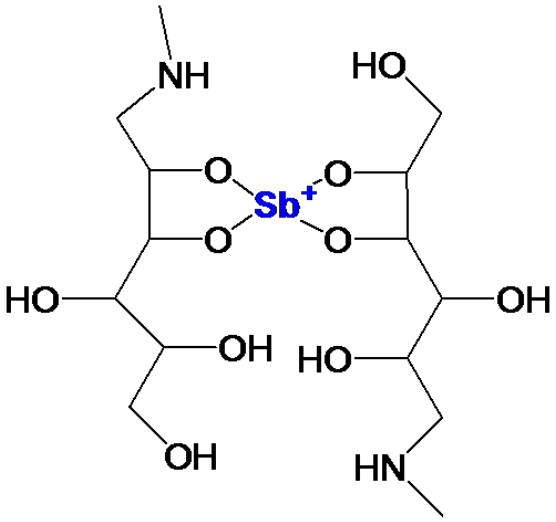

Figure 13: Structure of meglumine antimoniate

Studies conducted at the International Zoonoses Center (CIZ), in Quito-Ecuador, have shown that fluoroquinolones present an inhibitory effect on the growth of promastigotes of *Leishmania Mexicana*. Enrofloxacin has the highest anti-leishmanial activity with a MIC, NIC, and IC50 of 7210uM, 234,9uM, and 1498uM, respectively. (Esteves & Santamaría, 2018)

The purpose of this thesis is to develop a cellulose-based hydrogel loaded with enrofloxacin that can be used as an alternative topical treatment for CL improving the

drug delivery of the enrofloxacin with a controlled release, thus, reducing the adverse effects and preventing the drug resistance.

3. HYPOTHESIS AND OBJECTIVES

3.1 Hypothesis

Hydrogels made of commercial cellulose fibers can be used as enrofloxacin delivery system against Leishmaniasis

3.2 General objective

To measure the anti-leishmanial activity of a cellulose-based hydrogel loaded with enrofloxacin.

Specific objectives:

- To synthesize cellulose-based hydrogels loaded with enrofloxacin
- To characterize the hydrogels using SEM and AFM techniques
- To develop the drug release profile of the hydrogels using the Franz Cell.
- To measure the anti-leishmanial activity of the hydrogels using the Franz Cell.

Scheme 1. Flow- chart of the objectives of this investigation

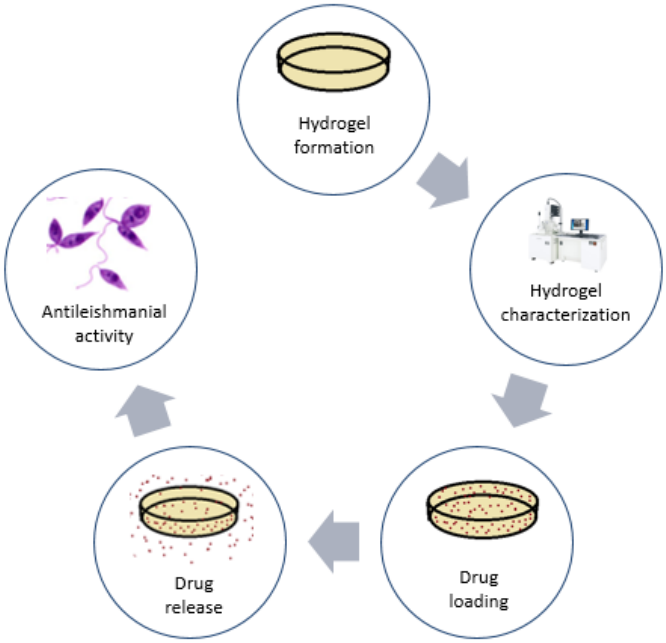

4. METHODS

4.1 Materials

Table 3: Materials

Raw material	**Cellulose fibers: from Sigmacell. (Cellulose type 20, 20um.)** **Enrofloxacin**
Reagents	Solution A: 6%NaOH 4%Urea filtered with a membrane of 0.2um Buffer A: 0.1M of Citric acid, sodium citrate pH=5.2 Ethanol 99% purity
Culture medium	Schneider medium with 10% of fetal serum bovine
Material	Petri dishes, six-well cell culture reservoir, falcon tube, gloves, 2um filter, and beakers.
Equipment	Freezer, incubator, oven, pipets, UV-Vis spectrophotometer, analytic balance, vortex, autoclave.

*All the reagents and materials must be sterilized to all the processes.

4.2 Hydrogel Preparation

For the hydrogel synthesis, the method described by Chang and collaborators, using NaOH-Urea aqueous solution, was used applying some modifications (Chang, Zhang, Zhou, Zhang, & Kennedy, 2010). The method is described in the following scheme:

Scheme 2. NaOH/Urea method

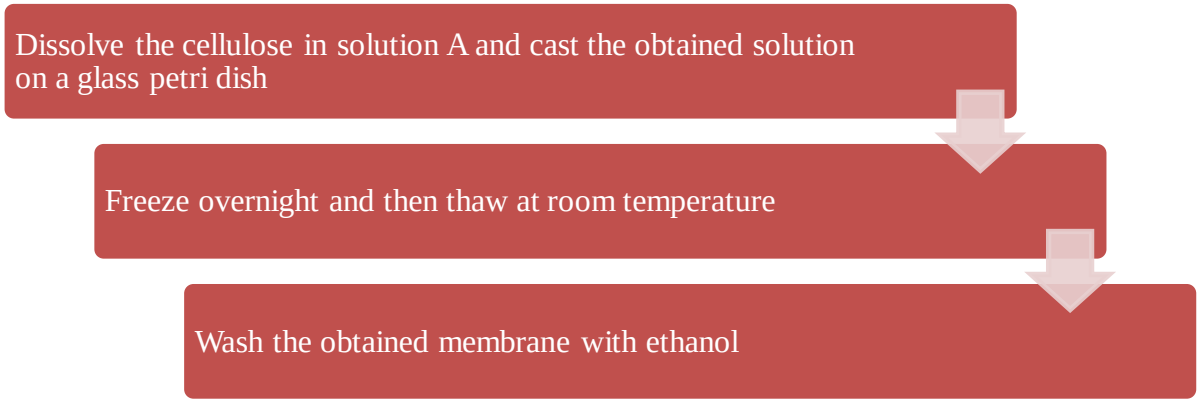

4.3 Characterization

4.3.1 Cellulose fibers characterization

Fourier-transform infrared spectroscopy (FTIR) was used to determine the functional groups of the cellulose fibers and to verify that there is no residual content of other molecules such as hemicellulose or lignin. MIRA 3 (TESCAN, CZ) field emission scanning electron microscope (FEG- SEM) was used to study the porosity, morphology, and size of the cellulose fibers. The crystallinity of the cellulose fibers was analyzed through X-Ray Diffraction on an EMPYREAN diffractometer (PANalytical, NL) in a Bragg-Brentano configuration at 40 kV and 45 mA and monochromatic X Rays of Cu K-α wavelength (λ = 1.541 Å) using a Ni filter. (Bravo et al., n.d.; Paula, Guambo, & Alexis, 2019)

4.3.2 Hydrogel characterization

For the hydrogel characterization, the atomic force microscopy technique (AFM) was used to determine topographical features and mechanics at the nanoscale. (Iturri & Toca-Herrera, 2017). In addition, SEM was used to determine the porosity, morphology, and size of the hydrogel.

4.3.3 Hydrogel degradation

In this work, the hydrogel degradation was measured in sterile water. First, 4 ml of the hydrogel coagulated in ethanol were weighed and placed in 250 mL of water at a temperature of 37 °C in the incubator. The measurements were taken basis to evaluate the weight loss of the hydrogel; this process was carried out at 0, 1, 24, 48, 72, 120, and 168 hours.

4.4 Release profile

First, the enrofloxacin loading was made in solution A before the dissolution of the cellulose fibers. For the release profile, Buffer A of a pH value of 5.2 was used to mimic the pH of the skin.

The calibration curve of enrofloxacin was made with a 10ml stock solution of 0.25mg/ml of enrofloxacin in buffer A; then dilutions were performed to obtain the standards of 2, 4, 6, 8, 10, 12, 16, 18, 20, 22, 24, 26, 28, 30 ug/ml. The samples were measured in the spectrophotometer at 280nm using as blank the Buffer A. The release profile measurements were performed using the Franz Cell, the assays with this type of

cells are appropriated to evaluate the percutaneous penetration of drugs (transdermic or topic). Llanga, D, provided the method and the Franz Cell; we perform several modifications applied to hydrogels and Leishmaniasis study. (Llanga, 2019)

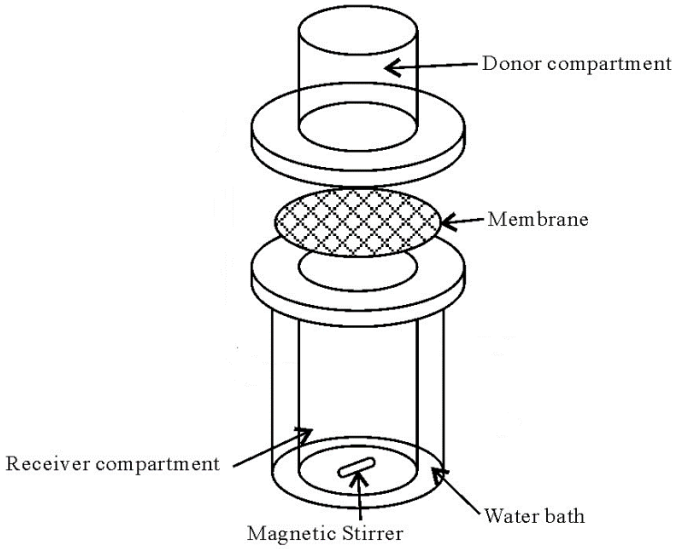

Figure 14: Scheme of Franz Cell

Donor compartment: 4ml hydrogel loaded with a concentration of 0.5mg/ml enrofloxacin. The hydrogel was made in a six-well cell culture receiver and coagulated for 5 minutes in ethanol.

Membrane: Cellophane membrane previously immersed for 5 minutes in distilled water.

Figure 15: Optimized Franz Cell by Llanga, D.

Scheme 3: In-vitro transdermal permeability test

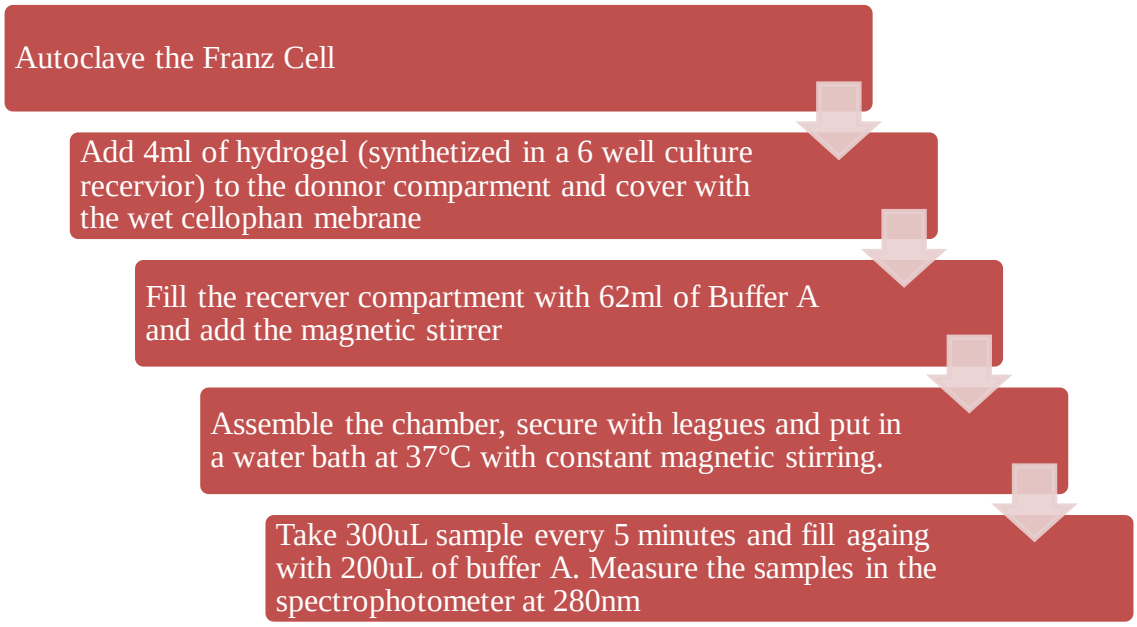

4.4.1 Transdermal permeability study

For the determination of the transdermal permeability, the method described by Llanga, D, and Lasso, J, was used to determine the area under the curve, permeability coefficient, and the latent period. (Lasso & Ruiz, 2017; Llanga, 2019). The wet cellophane membrane was used as the artificial membrane to mimic the skin.

Table 4: Parameters for the transdermal permeability

	Transdermal permeability assay	
Parameters	Area under the curve (AUC)	mg * min / cm^2
	Permeability coefficient (K_p)	cm^2/min
	Latent period (T_L)	min

4.4.2 Release Kinetics

Using linear regression in R software, and based on goodness of fit using the coefficient of determination (r^2), adjusted coefficient of determination (R^2), and the Akaike information criterion (AIC), the data obtained with the Franz Cell was analyzed using the mathematical models described in *Table 2* to determine the drug delivery release kinetics of the enrofloxacin from the hydrogel matrix.

The Akaike information criterion (AIC) is a tool to estimate the likelihood of a model to predict future values based on in-sample fit. The best model has the lowest AIC value among all the other models. (Akaike, 1974)

4.5 Anti-Leishmanial test of hydrogels

For this test, the same principle of the Franz Cell was used.

First, the Franz Cell was autoclaved, and the cellophane membrane was sterilized using a UV light for 5 minutes and then submerged in sterile water for 5 minutes. The receiver compartment was filled 62 ml of a culture of $1x10^6$ of promastigotes of *Leishmania mexicana* in Schneider medium with 10% of Fetal Bovine Serum. The donor compartment: 4ml of hydrogel with the IC50 concentration of enrofloxacin 1498uM (Esteves & Santamaría, 2018). The hydrogel was made in a six-well cell culture receiver and coagulated for 5 minutes in ethanol. Finally, the promastigotes were observed on the microscope before and after an incubation of 24 hours at 25°C.

In addition, cellulose-based hydrogels beads were performed using the same method of synthesis described before. 2ml of hydrogel beads containing the IC50 concentration (1490uM) were washed with acid to obtain an acid pH=6. These beads were cast in 10 ml of a culture of $1x10^6$ of promastigotes of *Leishmania mexicana* in Schneider medium with 10% of Fetal Bovine Serum in a 50 ml Falcon Tube.

4.6 Statistics

All the experiments are done by triplicate, and the results are presented with the mean ± standard deviation

5. RESULTS, INTERPRETATION, AND DISCUSSION

5.1 Characterization

5.1.1 Fibers Characterization

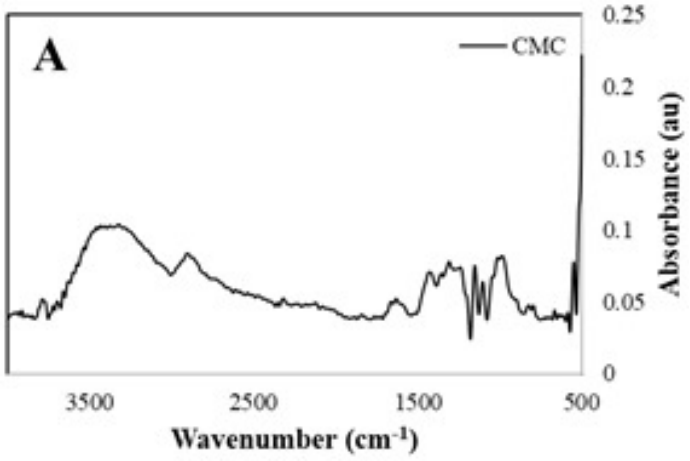

Figure 16: FTIR analysis of cellulose fibers

The FTIR spectra of the cellulose fibers present the characteristic peaks for cellulose; C-C, C-OH, C-H ring, and side group vibration bands at ~1000 cm^{-1}, C-O-C glycosidic ether band at ~1105 cm^{-1}. Finally, it can be observed at ~1300 cm^{-1} CH_2 rocking vibrations, at ~1625 cm^{-1} the OH bending of absorbed water, at ~2900 cm-1 sp3 C-H stretching, and at ~ 3300 cm^{-1} the OH stretching frequencies.

Figure 17: SEM analysis of cellulose fibers

The SEM analysis shows a fiber morphology of the cellulose with a lack of porosity. Besides, the fibers have a length of ~100*um* and a width of ~20*um*.

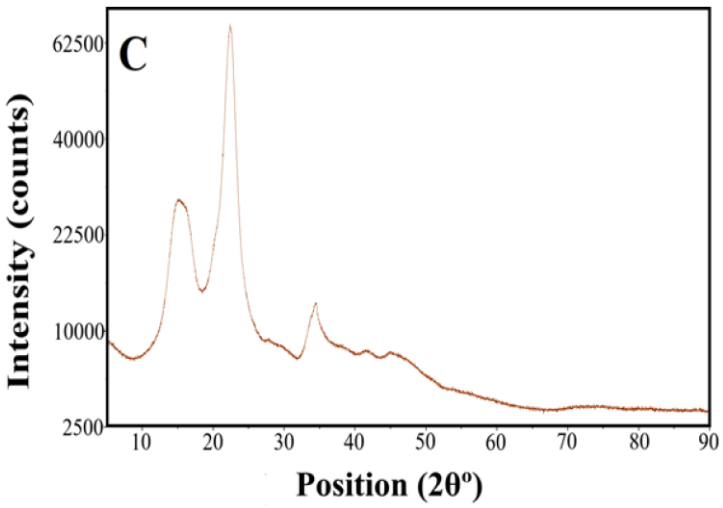

Figure 18: X-Ray Diffraction analysis of cellulose fibers

Finally, the X-Ray Diffraction of the cellulose fibers presents a crystallinity of 57.8%

5.1.2 Hydrogel Characterization

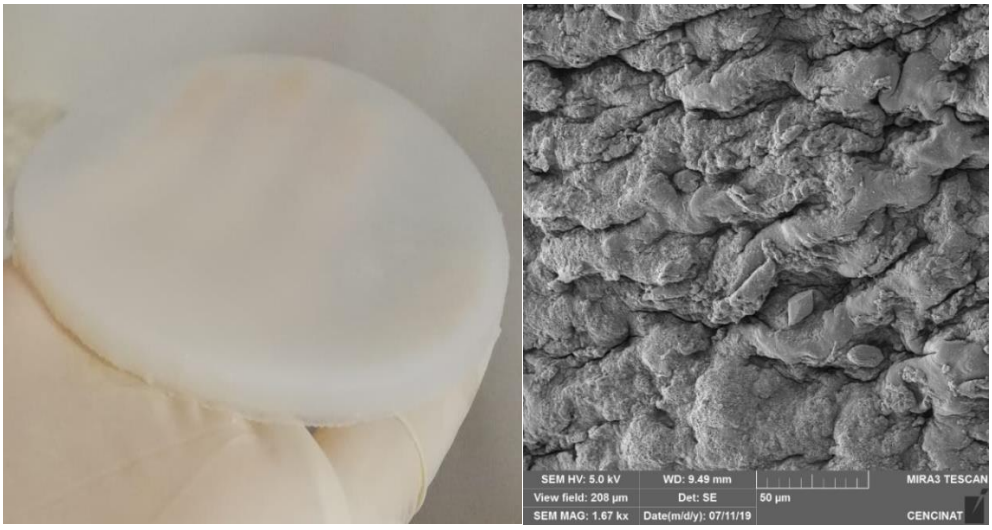

Figure 19: Obtained cellulose-based hydrogel and SEM characterization

During the gel manufacturing process, there were no inconveniences in the dissolution of the cellulose, producing a homogeneous white fluid.

In the organoleptic parameters, the hydrogel presents a solid and hard consistency similar to a membrane, white color, homogeneous, lump-free, and a slight ethanol smell. The pH of the hydrogel was measured with pH test strips; a pH value of 10 was obtained; however, this pH can be neutralized by baths with distilled water or acidic pH solutions.

The Scanning Electron Microscopy of the cellulose-based hydrogel presents an irregular morphology with a porous structure; also, it shows how the cellulose fibers are aligned to form the hydrogel.

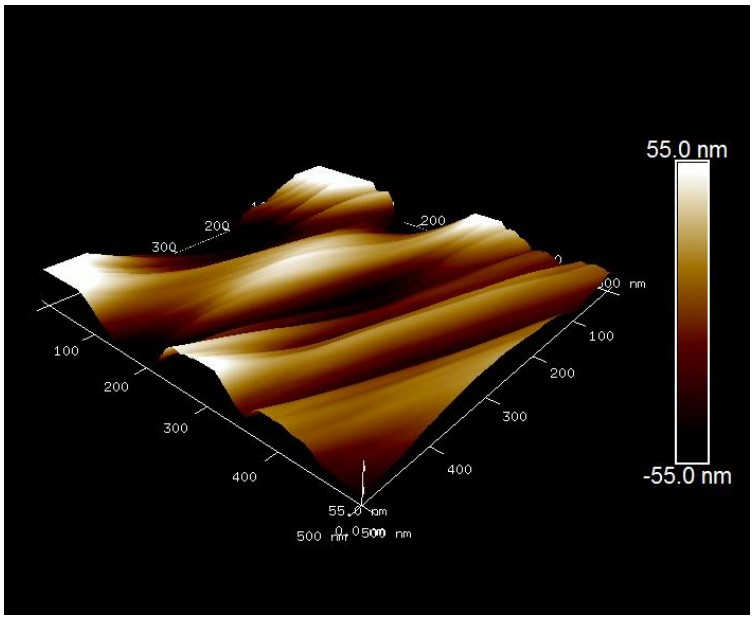

Figure 20: Atomic force microscopy of the cellulose-based hydrogel

The AFM analysis shows the topographical analysis of the hydrogel, a three-dimensional network undulating surface. No protrusions or hump-like regions are observed.

5.1.3 Hydrogel degradation

The degradation profile was made in water at 37°C; the experiment was done by triplicate, *Annex A* presents the detailed table of the results for each sample.

Table 5: Percentage of average weight remaining hydrogel in water

Time (hours)	Weight percentage (average)	Standard deviation
0	100,00	0,00
1	89,46	5,11
24	75,15	3,65
48	74,59	1,79
120	71,54	0,08
168	69,77	0,83
240	67,54	1,86

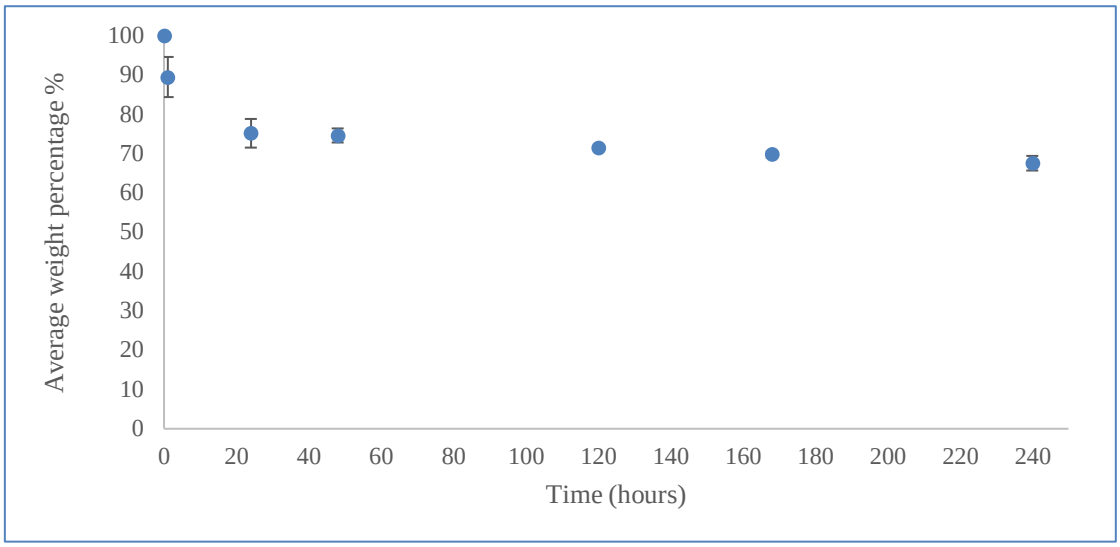

Figure 21: Percentage of hydrogel remaining after several hours in the water

The degradation of the hydrogel decays in the first two days (48 hours), 65% of the initial weight remains over time. After this time, there is no significant degradation of the hydrogel.

5.2 Release Profile

With the calibration curve, we obtain that the concentration [*ug/ml*] is the absorbance, measured at 280*nm*, divided by 0.0559 used in the calculation of the total enrofloxacin. *Annex B* presents in detail the data obtained.

Figure 22: Assembly of the hydrogel in the donor chamber of the Franz Cell with the cellophane membrane.

Figure 23: Franz Cell experimentation

The Franz Cell was assembled to ensure that the entire surface of the hydrogel covered with the membrane is in contact with the buffer A, giving a homogeneous enrofloxacin release over the surface of the hydrogel. The Franz Cell was opened every five minutes for 3 to 4 seconds to take samples to measure in the spectrophotometer.

5.3 Transdermal permeability study

Samples were taken every 5 minutes during 80 minutes (three repetitions), we determine the concentration of enrofloxacin in the receptor compartment, the amount and percentage of drug released from the hydrogel, and the amount of active substance per unit of area (*Q*). Q is the product of the multiplication of the concentration by the total volume of the receptor (62*ml*) divided for the total area of the membrane (9,621cm^2). *Annex C* shows the complete table with all the values of each sample, mean, and standard deviation. The concentration of the hydrogel is 0,5*mg/ml*, and the final volume of hydrogel was 4*ml*.

Table 6: Results of the enrofloxacin release

Time	Concentration in the receptor compartment [ug/ml]		Percentage of drug released from the hydrogel%		Amount of active substance per unit area (Q) [ug/cm2]	
	Mean	**S.D.**	**Mean**	**S.D**	**Mean**	**S.D.**
0	0,00	0,00	0,00	0,000	0,00	0,00
5	5,65	0,41	17,51	1,270	36,39	2,64
10	9,06	0,94	28,10	2,908	58,41	6,05
15	11,88	0,38	36,82	1,193	76,55	2,48

20	15,03	0,72	46,58	2,246	96,84	4,67
25	18,39	0,43	57,01	1,346	118,51	2,80
30	22,06	0,74	68,40	2,309	142,18	4,80
35	24,04	0,10	74,53	0,309	154,94	0,64
40	25,72	0,33	79,75	1,036	165,77	2,15
45	27,66	0,45	85,74	1,400	178,23	2,91
50	28,81	0,26	89,30	0,804	185,64	1,67
55	30,78	0,34	95,42	1,056	198,36	2,19
60	31,59	0,08	97,92	0,250	203,55	0,52
65	32,23	0,14	99,91	0,424	207,70	0,88
70	32,22	0,02	99,88	0,055	207,62	0,12
75	32,24	0,09	99,93	0,293	207,74	0,61
80	32,23	0,05	99,91	0,160	207,70	0,33

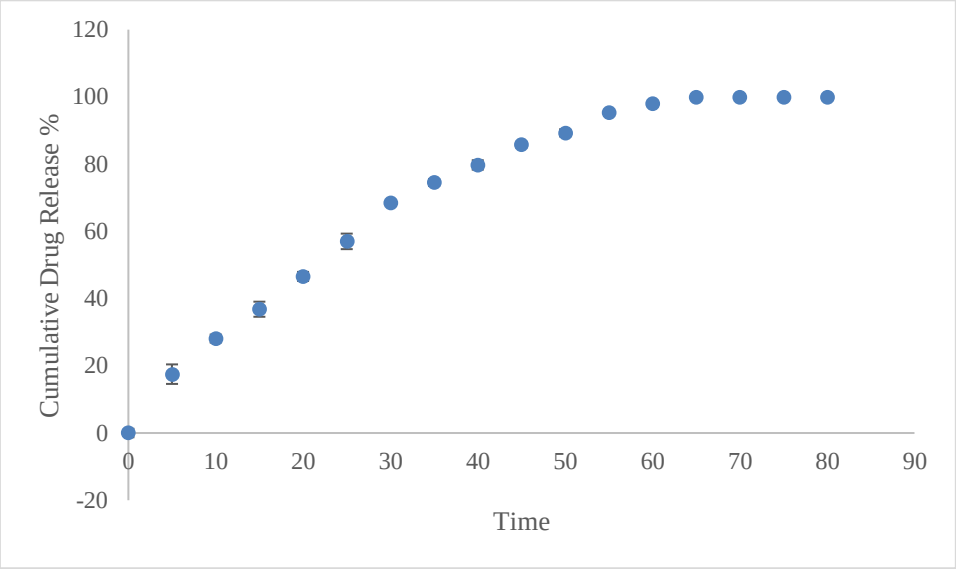

Figure 24: The in-vitro cumulative release profile of enrofloxacin in buffer A.

The behavior of the enrofloxacin release presents a controlled release from the hydrogel in the Franz Cell. The complete release was achieved within one hour, and 50% of the drug was released in the first 20-25 minutes. It is important to mention that 100% of enrofloxacin loaded in the hydrogel was released, and there is no loss of the antibiotic during the manufacturing process. For the next analysis, we take the first 60 minutes, which is when we obtain a 100% release of enrofloxacin.

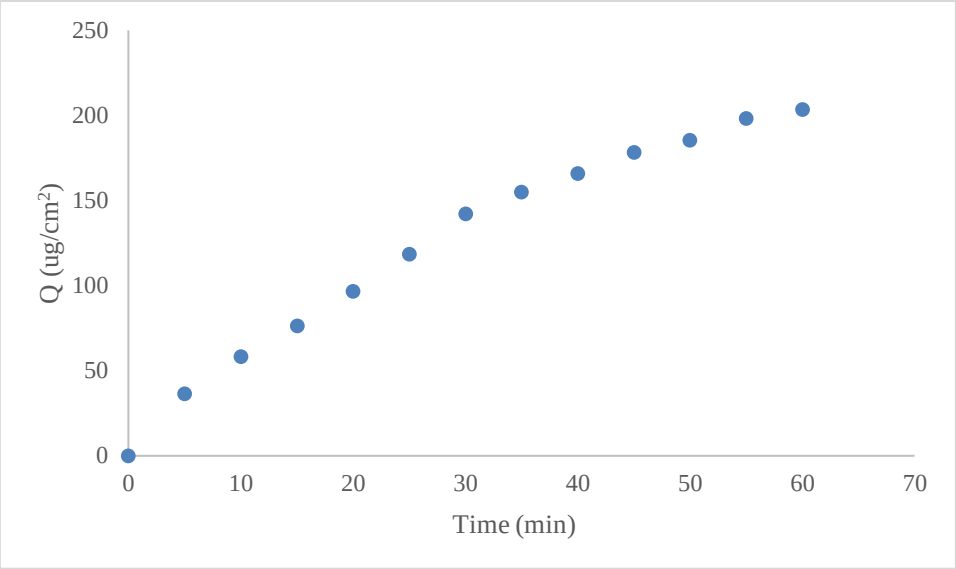

Figure 25: Amount of active substance per unit of area (Q) vs. time

In this figure, we can observe that there is a variation in the slope from the 35 minutes. To determine the transdermal permeability, we will use the time interval from zero to 30 minutes.

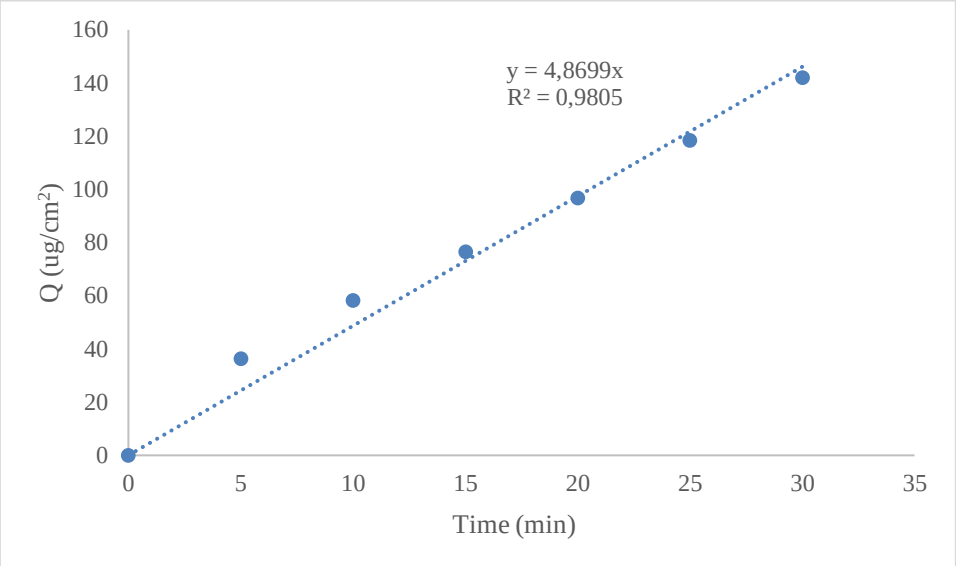

Figure 26: Q vs. time

Using linear regression, we obtain the equation *y=4,8699x* with a correlation coefficient of 0,9805. For the study of transdermal permeability, we took the slope as the transdermal flux (J)

$$J = 4{,}8699 \text{ ug}/\ (cm^2 * \text{min})$$

For the area under the curve, we use the following equation

$$AUC = \sum \left[\frac{Q_1 + Q_2}{2} * (t_2 - t_1) \right]$$

Equation 4: Area under the curve

Table 7: Area under the curve values

Time (min)	Q (mg/cm2)	AUC (ug*min /cm2)
0	0,00	0,00
5	36,39	90,98
10	58,41	237,00
15	76,55	337,39
20	96,84	433,46
25	118,51	538,36
30	142,18	651,72
35	154,94	742,80
40	165,77	801,78
45	178,23	860,00
50	185,64	909,67
55	198,36	960,01
60	203,55	1004,77
	Total	**7567,94**

For the determination of the permeability coefficient (K_p), we divide the transdermal flux (J) by ΔC, the concentration gradient of enrofloxacin that is approximately the concentration in the donor compartment 2000*ug*.

$$Kp = \frac{J}{\Delta C}$$

Equation 5: Permeability coefficient

Equation: transdermal permeability coefficient

$$Kp = \frac{4{,}8699 \ \frac{ug * cm^2}{min}}{2000\text{ug}} = 2{,}434x10^{-3} cm^2/min$$

5.4 Release Kinetics

Table 8: Evaluation of the mathematical methods used to describe the enrofloxacin release kinetics from the hydrogel matrix.

Model	r^2	Adjusted R^2	AIC
Zero Order	0,9633	0,9599	88,73
First Order	0,9158	0,9081	-7,93
Higuchi Model	0,9785	0,9766	81,75
Hixson–Crowell Model	0,9865	0,9853	-12.87
Korsmeyer-Peppas Model	0,5871	0,5496	14,27

* *Annex E* shows the graphs of the analyzed model.

Based on the Akaike information criterion and the coefficients of determination, the best models that describe the enrofloxacin release are the first-order kinetics and the Hixon-Crowell model. For the cellulose-based hydrogels loaded with erofloxacin, we determine that the release kinetics fits the first order release model because this method is widely used to describe the release kinetics of several soluble drugs in porous materials, which is the case of the enrofloxacin that is soluble in buffer A and it is released from a porous cellulose-based hydrogel. (Baishya, 2017; Shaikh et al., 2015). On the other hand, the Hixon-Crowell model describes the kinetics release of systems where there is change in surface area and diameter of particle, matrix, or tablet, thus, it is not the case of our cellulose-based hydrogel, because the enrofloxacin is released from the matrix without any change on the morphology and size of the hydrogel.

Equation 6: First Order Kinetic Model

$$LogC = LogC_o - Kt/2.303$$

C_o: Initial concentration of drug

K: First order constant

t: time

The data obtained are plotted as the logarithm of the cumulative percentage drug remaining versus time, *figure 36*, which yield a straight line with slop=K/2.303. In the

linear regression we obtain the following equation $y = -0,0249x + 2,1564$. As a result, the first order constant (K) has a value of 0,057 min^{-1}.

It is the first time that cellulose-based hydrogels are designed for enrofloxacin controlled drug delivery. However, several hydrogels of different polymers have been described for the release of enrofloxacin.

Vilches and collaborators (2002), describes the release kinetics of fluoroquinolones from carbomer hydrogels using Franz Cell in a 0,9% NaCl solution as receptor media. The model that best describes the release kinetics was zero-order. The 35% of the drug was released in 6 hours in NaCl medium and 5% of the drug was released in water medium. (Vilches et al., 2002)

Khanamani Falahatipour and collaborators (2016), describes a chitosan-based hydrogel for injectable delivery of enrofloxacin. The hydrogels can release all the drug in 120 hours and it is a big difference with the cellulose-based hydrogels that release the drug within one hour. For the drug release, the best-fit model was Korsmeyer-Peppas. (Khanamani Falahatipour et al., 2017)

5.5 Anti-leishmanial activity

The promastigotes of *Leishmania mexicana* were counted using the Neubauer chamber to corroborate that we have a concentration of $1x10^6$ cells. In addition, the cell culture was studied under the microscope to verify the mobility and the shape of the promastigotes to ensure that the cell culture is alive.

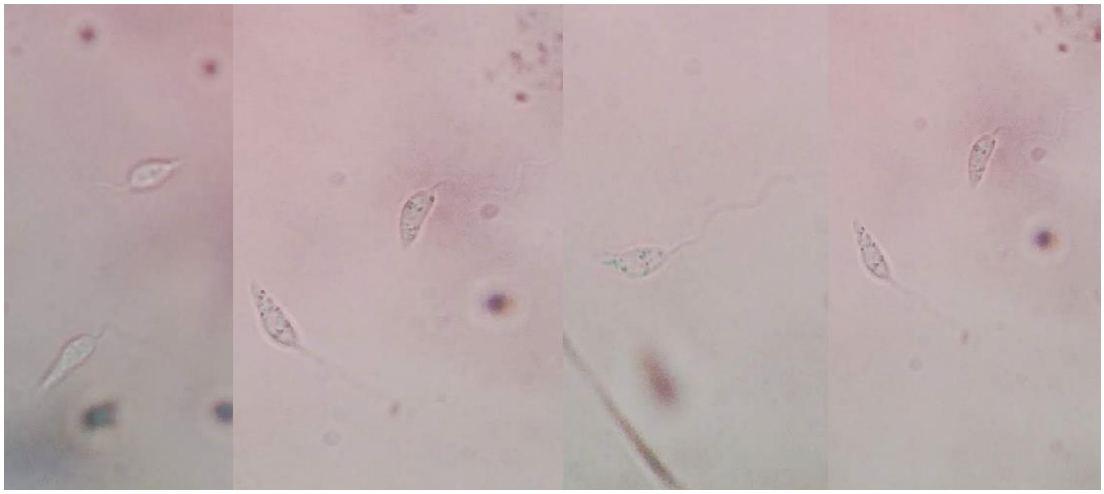

Figure 27: Promastigotes of Leishmania Mexicana under optic microscope 100X

After all the verifications of the promastigotes cell culture, 62 ml of the culture were cast in the reservoir chamber of the Franz Cell and cover with the donor chamber with the hydrogel loaded with an enrofloxacin concentration of 1498uM. The Franz Cell was incubated at 25°C for 24 hours. *Figure 28* shows the Franz Cell before incubation to ensure that there is no contamination or precipitations.

Figure 28: Franz Cell with the promastigotes cell culture before incubation. Time zero.

After the 24 hours of incubation, we observed a precipitate on the cell culture in the receptor chamber. These precipitations can be due to the degradation of the hydrogel or the formation of salts due to the acid pH of the medium and the basic pH of the hydrogel, among other reasons. The white precipitate can be observed in *Figure 29.*

Figure 29: Promastigotes cell culture after 24 hours of incubation with the hydrogel. A white precipitate can be observed. Optic microscopy 100X.

After the 24 hours, several samples of the promastigotes cell culture were taken and analyzed under the microscope. As a result, we can observe crystals of enrofloxacin and cellulose particles result of the hydrogel degradation; however, just a few *Leishmania* were found the medium without mobility and with a circular shape. No bacterial contamination was observed under the microscope. *Figure 30* shows the medium analyzed on the microscope.

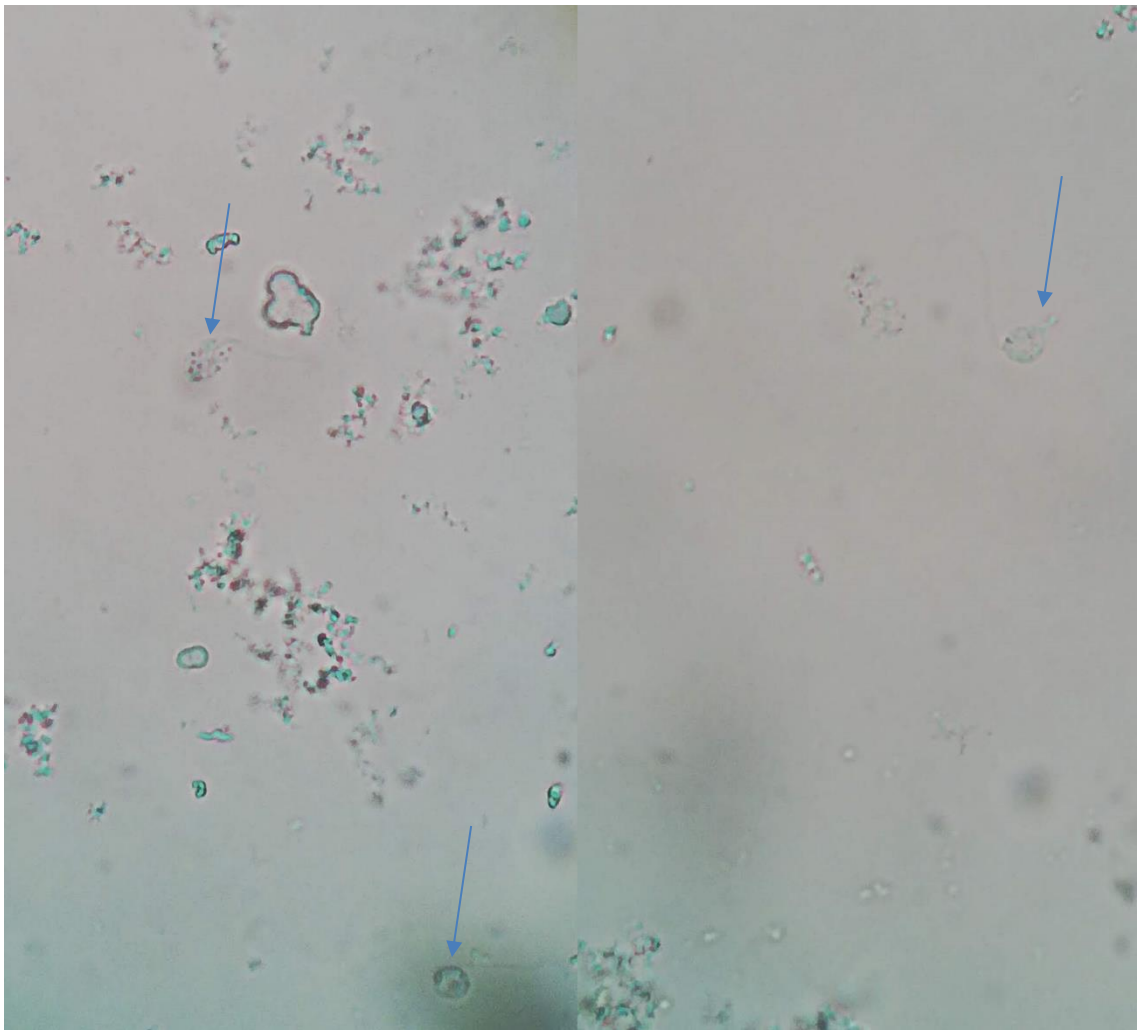

Figure 30: Medium of promastigotes of Leishmania Mexicana after 24 hours of incubation. Blue arrows: Leishmania mexicana

In addition, to determine that there is no toxicity of the cellulose fibers, 5ml of $1x10^6$ promastigotes of *Leishmania Mexicana* were incubated at 25°C with one gram of cellulose for 24 hours. As a result, normal growth of the parasites was observed; as a result, cellulose fibers do not present toxicity for the promastigotes of *L. mexicana*.

On the other hand, the cellulose-based beads of hydrogel was performed, *figure 31* shows the resulting beads with a perfect spherical form and an approximated diameter of 1mm. The beads presents a pH value of six.

Figure 31: Cellulose-based hydrogel beads

First, 2 ml of hydrogels beads without the enrofloxacin were incubated for 24 h in 10 ml of promastigotes cell culture of *L. Mexicana* to corroborate that the cellulose-based hydrogel beads does not present a toxic effect on the parasites culture. After the 24 hours, the culture were observed under the microscope and counted in the Neubauer chamber, as a result, no dead parasites was found and $7{,}1x10^6$ parasites was count that fits in the growth curve described by Esteves & Santamaría, 2018.

Moreover, a 10 ml of promastigotes cell culture of *L. mexicana* with a concentration $1x10^6$ cell were incubated for 24 hours at 25°C with 2ml of hydrogel beads loaded with a concentration of 1498uM of enrofloxacin. After the 24 hours, the culture was observed under the microscope and we can observe that most of the *L. mexicana* parasites were found circular and without movement assuming cell dead (*Figure 33*). In addition, no formation of precipitates was observed in the culture or under the microscope.

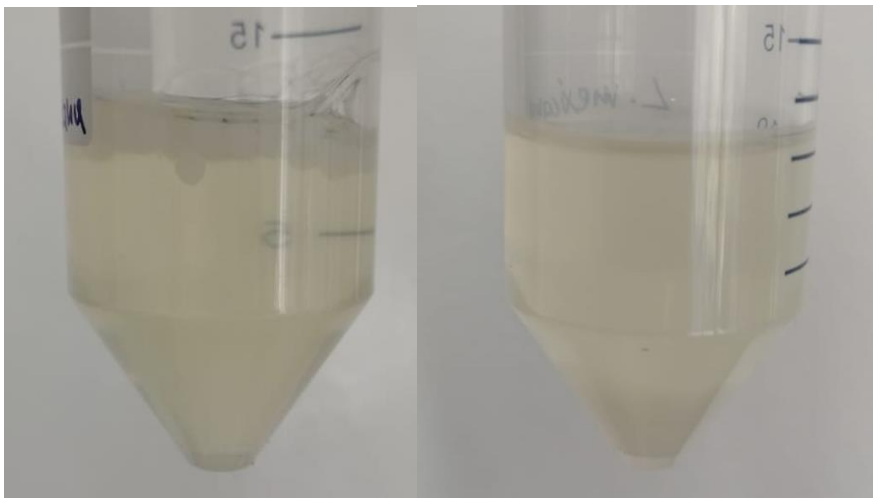

Figure 32: L. mexicana with beads loaded with enrofloxacin. Left: concentration 1x10^6 parasites at time zero. Right: 24 hours of incubation at 25°C

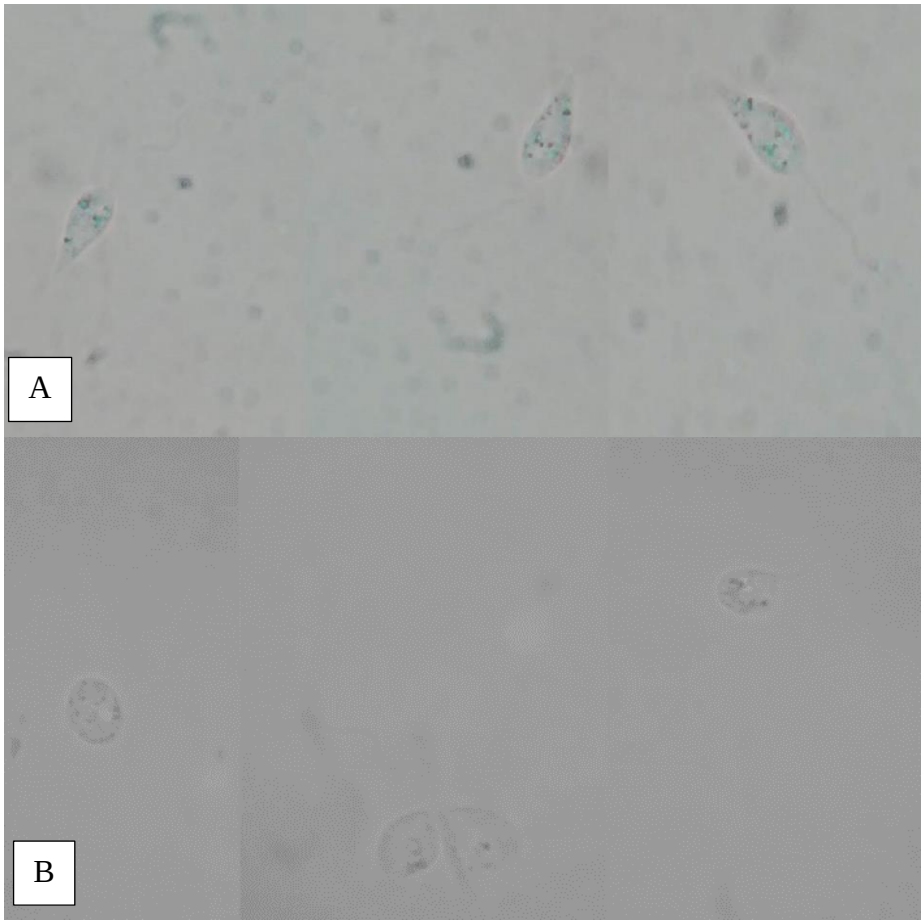

Figure 33: L. Mexicana observed under the microscope (100X) after 24 hours of incubation of hydrogel beads. A) Without enrofloxacin. B) Loaded with enrofloxacin

6. CONCLUSIONS AND RECOMMENDATIONS

Cellulose-based hydrogels were successfully synthesized and loaded with enrofloxacin using the NaOH-Urea method. The cellulose fibers present a micrometrical scale and a crystallinity of 57.8%. The hydrogels present a white color and are solid membranes that allow easy manipulation to be applied in the body without any break, 10 pH; SEM shows an irregular porous morphology while AFM shows an undulating surface. Regarding the hydrogel degradation, it maintains 65% of its weight over time.

By the transdermal permeability assay in-vitro, using the Franz Cell and cellophane membrane, it was obtained that the release profile of the enrofloxacin presents a controlled release of one hour with a 100% release of the hydrogel following first-order release kinetics. The transdermal parameters: transdermal flux (*J*), area under the curve of the permeability profile (*AUC*), and permeability coefficient (K_p), presented a value of 4,8699 $ug/(cm^2*min)$, 7567,94 $ug*min/cm^2$, and 2,434x10^{-3} cm^2/min.

The cellulose-based hydrogels using the Franz Cell presented a high effectivity against promastigotes of *L. mexicana*; however, the formation of a precipitate in the promastigotes medium does not provide concluding results; but despite that, cellulose has no toxicity for the parasites. More studies have to be done to provide concluding results regarding the anti-leishmanial activity. On the other hand, the cellulose-based hydrogel beads loaded with enrofloxacin provide excellent results in the anti-leishmanial test with no toxic effects of precipitations that affects the normal growth of the parasites, giving as a result no interference of chemicals and a total anti-leishmanial activity of the enrofloxacin.

Finally, cellulose-based hydrogels are a promising tool for the treatment of neglected diseases such as Leishmaniasis, which have toxic and long treatments, thus, improving the quality of life of the patients and increase patient compliance and adherence to the treatment.

Future work and recommendations

It is essential to improve the design of Franz's diffusion cell, in terms of its operability, to avoid operational errors and keep the cell always closed.

It is necessary to perform more transdermal permeability studies by varying the membranes, whether natural or synthetic.

It is the first time that cellulose-based hydrogels are used for drug delivery against leishmaniasis, the reason why we need to do more research to determine the cause of the formation of the precipitate in the *Leishmania* culture and why in the release study there was no precipitation. In addition, we are working on the development of a cellulose-based hydrogel with a neutral or slightly acid pH to prevent the precipitation due to the possible salt formation in the promastigote assay and to improve patient compliance and prevent possible toxic effects of the hydrogel. Furthermore, we are evaluating the antibacterial activity of the hydrogels at different pH.

On the other hand, the group of the Centro Internacional de Zoonosis is working in the study of the effect of the enrofloxacin in infected macrophages and amastigotes of *L. mexicana* having promising results, so the next step is to evaluate the hydrogels loaded with enrofloxacin in the infected macrophages.

Finally, we are also working on the development of cellulose-based hydrogels with natural cellulose fibers extracted from Ecuadorian plants that will be used for comparative assays in the release profile, transdermal permeability, and anti-leishmanial activity.

7. REFERENCES

Ahmed, E. M. (2015). Hydrogel: Preparation, characterization, and applications: A review. *Journal of Advanced Research*, *6*(2), 105–121. https://doi.org/10.1016/j.jare.2013.07.006

Akaike, H. (1974). A new look at the statistical model identification. *IEEE Transactions on Automatic Control*, *19*(6), 716–723. https://doi.org/10.1109/TAC.1974.1100705

Aulton, M. E. (2004). *La Ciencia del Diseño de Formas Farmacéuticas* (Second). Elsevier.

Baishya, H. (2017). Application of Mathematical Models in Drug Release Kinetics of Carbidopa and Levodopa ER Tablets. *Journal of Developing Drugs*, *06*(02). https://doi.org/10.4172/2329-6631.1000171

Bravo, I., Figueroa, F., Swasy, M., Attia, M., Ateia, M., Encalada, D., & Vizuete, K. (n.d.). *Decontamination of VOC Pollutants with Cellulose from Biodiversity*. 1–16.

Bruschi, M. (2015). Mathematical models of drug release. In *Strategies to Modify the Drug Release from Pharmaceutical Systems* (pp. 63–86). https://doi.org/10.1016/B978-0-08-100092-2.00005-9

Carrillo, K., & Miranda, M. (2018). *LESIONES CUTÁNEAS POR LEISHMANIASIS, CARACTERIZACIÓN Y RESPUESTA AL TRATAMIENTO LOCAL Y SISTÉMICO EN LA POBLACIÓN DEL NOROCCIDENTE DE PICHINCHA DESDE ENERO 2014 HASTA JULIO 2017*. Pontificia Universidad Católica del Ecuador.

Chang, C., Zhang, L., Zhou, J., Zhang, L., & Kennedy, J. F. (2010). Structure and properties of hydrogels prepared from cellulose in NaOH/urea aqueous solutions. *Carbohydrate Polymers*, *82*(1), 122–127. https://doi.org/10.1016/j.carbpol.2010.04.033

Dickson, L. (2019). Ficks first law of diffusion. In *Annalen der Physik* (Vol. 170, p. 59). Retrieved from https://chem.libretexts.org/Bookshelves/Physical_and_Theoretical_Chemistry_Textbook_Maps/Supplemental_Modules_(Physical_and_Theoretical_Chemistry)/Kinetics/Diffusion

Esteves, L., & Santamaría, J. (2018). *EFECTO DE LAS FLUOROQUINOLONAS SOBRE LAS TOPOISOMERASAS TIPO II EN TRYPANOSOMATIDAE*. Universidad Central del Ecuador.

Estevez, T., Aguilera, A., Saez, A., & Hardy, E. (2000). Diseno y validacion de una celda de difusion para estudios de liberacion in vitro de biomoleculas.

Biotecnologia Aplicada, *17*(3), 187–190.

Eucerin. (n.d.). Skin pH. Retrieved from https://int.eucerin.com/about-skin/basic-skin-knowledge/skins-ph

Hashiguchi, Y., Velez, L. N., Villegas, N. V., Mimori, T., Gomez, E. A. L., & Kato, H. (2017). Leishmaniases in Ecuador: Comprehensive review and current status. *Acta Tropica*, *166*, 299–315. https://doi.org/10.1016/j.actatropica.2016.11.039

Heinze, T. (2015). *Cellulose: Structure and Properties*. https://doi.org/10.1007/12_2015_319

Himanshi Tanwar * and Ruchika Sachdeva. (2016). Transdermal Drug Delivery System: a Review | International Journal of Pharmaceutical Sciences and Research. *International Journal of Pharmaceutical Sciences and Research*, *7*(6), 2274–2290. https://doi.org/10.13040/IJPSR.0975-8232.7(6).2274-90

Iturri, J., & Toca-Herrera, J. L. (2017). Characterization of cell scaffolds by atomic force microscopy. *Polymers*, *9*(8). https://doi.org/10.3390/polym9080383

Kabir, S. M. F., Sikdar, P. P., Haque, B., Bhuiyan, M. A. R., Ali, A., & Islam, M. N. (2018). Cellulose-based hydrogel materials: chemistry, properties and their prospective applications. *Progress in Biomaterials*, *7*(3), 153–174. https://doi.org/10.1007/s40204-018-0095-0

Khanamani Falahatipour, S., Rasooli, A., Hosseinzadeh Ardakani, Y., Akbari Javar, H., Kiani, K., & Zahraee Salehi, T. (2017). Preparation and in vitro evaluation of a novel chitosan-based hydrogel for injectable delivery of enrofloxacin. *Iranian Journal of Veterinary Medicine*, *11*(1), 31–47. https://doi.org/10.22059/ijvm.2017.60305

Lasso, J., & Ruiz, J. (2017). *OPTIMIZACIÓN METODOLÓGICA PARA ESTUDIOS DE PERMEABILIDAD in vitro EMPLEADO LOS MODELOS DE CELDA DE FRANZ HORIZONTAL Y VERTICAL*. Universidad ICESI.

Leyva, S., & Leyva, E. (2008). Fluoroquinolonas. Mecanismos de acción y resistencia, estructura, síntesis y reacciones fisicoquímicas importantes para propiedades medicinales. *Sociedad Quimica DeMexico*.

Lizondo, M., Pons, M., Gallardo, M., & Estelrich, J. (1997). Physicochemical properties of enrofloxacin. *Journal of Pharmaceutical and Biomedical Analysis*, *15*(12), 1845–1849. https://doi.org/10.1016/S0731-7085(96)02033-X

Llanga, D. (2019). *Determinación de la influencia de la concentración de quitosano en la permeabilidad transdérmica in vitro de un gel de ácido salicílico empleando*

celdas de difusión de Franz. Universidad Central del Ecuador.

Ministerio de Salud Pública del Ecuador. (2019). ENFERMEDADES TRANSMITIDAS POR VECTORES INFORME LESHMANIASIS.

National Center for Biotechnology Information. (n.d.). Enrofloxacin. Retrieved from https://pubchem.ncbi.nlm.nih.gov/compound/Enrofloxacin

Paula, M., Guambo, R., & Alexis, F. (2019). *Fibras Vegetales Naturales para Aplicaciones en Sutura Quirúrgica*. Yachay Tech University.

Perm Gear. (n.d.). Franz Cell. Retrieved from https://permegear.com/franz-cells/

SafeHair. (n.d.). Skin Barriers. Retrieved from https://www.safehair.eu/trainee/what-you-should-know/layers-and-multitasking/skin-barriers/

Shaikh, H. K., Kshirgagar, R. V., & Patil, S. G. (2015). MATHEMATICAL MODELS FOR DRUG RELEASE CHARACTERIZATION. *WORLD JOURNAL OF PHARMACY AND PHARMACEUTICAL SCIENCES*, *4*(04), 324–338.

Uzcanga, G., Lara, E., Gutiérrez, F., Beaty, D., Beske, T., Teran, R., … Poveda, A. (2017). Nuclear DNA replication and repair in parasites of the genus Leishmania : Exploiting differences to develop innovative therapeutic approaches. *Critical Reviews in Microbiology*, *43*(2), 156–177. https://doi.org/10.1080/1040841X.2016.1188758

Vilches, A. P., Jimenez-Kairuz, A., Alovero, F., Olivera, M. E., Allemandi, D. A., & Manzo, R. H. (2002). Release kinetics and up-take studies of model fluoroquinolones from carbomer hydrogels. *International Journal of Pharmaceutics*, *246*(1–2), 17–24. https://doi.org/10.1016/S0378-5173(02)00333-2

World of Health Organization. (2018). Status of endemicity of cutaneous leishmaniasis Data by country.

World of Health Organization. (2019). Leishmaniasis. Retrieved from https://www.who.int/es/news-room/fact-sheets/detail/leishmaniasis

Zakharova, L., Pashirova, T., Kashapov, R., Gabdrakhmanov, D., & Sinyashin, O. (2017). Drug delivery mediated by confined nanosystems: structure-activity relations and factors responsible for the efficacy of formulations. In *Nanostructures for Drug Delivery* (pp. 749–806). https://doi.org/10.1016/B978-0-323-46143-6.00024-5

Zsikó, S., Csányi, E., Kovács, A., Budai-Szűcs, M., Gácsi, A., & Berkó, S. (2019). Methods to evaluate skin penetration in vitro. *Scientia Pharmaceutica*, *87*(3). https://doi.org/10.3390/scipharm87030019

8. ANNEXES

Annex A: Complete table with the data obtained from the degradation test in water

time (hours)	Weight (grams)					Weight Percentage %				
	Sample 1	Sample 2	Sample 3	Mean	Standard deviation	Sample 1	Sample 2	Sample 3	Mean	Standard deviation
0	5,05	4,92	5,11	**5,03**	**0,10**	100,00	100,00	100,00	**100,00**	**0,00**
1	4,81	4,08	4,60	**4,50**	**0,38**	95,34	82,88	89,98	**89,46**	**5,11**
24	4,00	3,73	3,60	**3,78**	**0,20**	79,29	75,81	70,42	**75,15**	**3,65**
48	3,88	3,66	3,71	**3,75**	**0,12**	76,89	74,37	72,54	**74,59**	**1,79**
120	3,62	3,52	3,65	**3,60**	**0,07**	71,64	71,54	71,44	**71,54**	**0,08**
168	3,55	3,46	3,51	**3,51**	**0,04**	70,35	70,37	68,60	**69,77**	**0,83**
240	3,46	3,40	3,32	**3,39**	**0,07**	68,63	69,10	64,95	**67,54**	**1,86**

Annex B: Complete table with the data obtained for the calibration curve of enrofloxacin in buffer A.

Concentration (ug/ml)	Sample 1	Sample 2	Sample 3	Mean	Standard Deviation
2	0,092	0,092	0,090	0,091	0,001
4	0,203	0,213	0,210	0,209	0,005
6	0,343	0,334	0,336	0,338	0,005
8	0,446	0,458	0,451	0,452	0,006
10	0,559	0,543	0,544	0,549	0,009
12	0,681	0,659	0,705	0,682	0,023
14	0,812	0,782	0,780	0,791	0,018
16	0,931	0,892	0,897	0,907	0,021
18	1,026	1,042	1,012	1,027	0,015
20	1,149	1,126	1,125	1,133	0,014
22	1,241	1,227	1,214	1,227	0,014
24	1,302	1,312	1,322	1,312	0,010
26	1,444	1,449	1,458	1,450	0,007
28	1,582	1,549	1,566	1,566	0,017
30	1,687	1,653	1,677	1,672	0,017

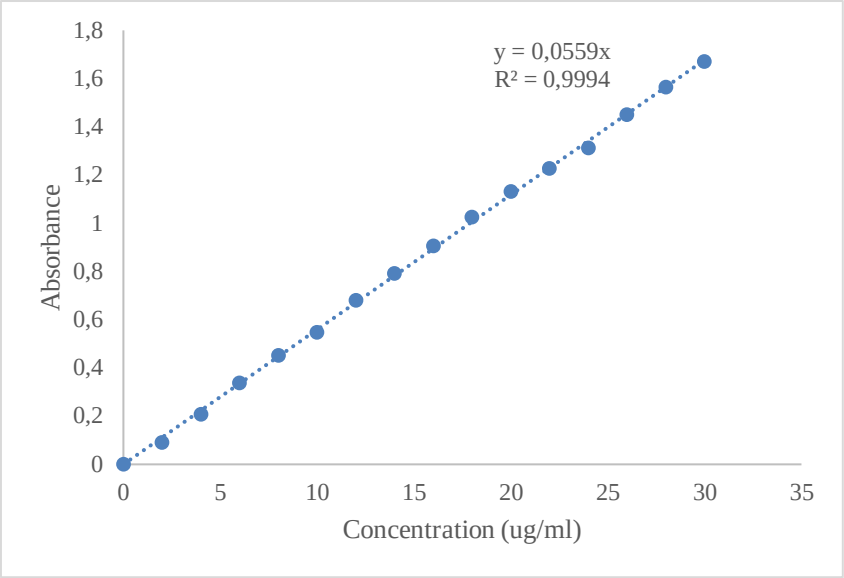

Figure 34: Calibration curve of enrofloxacin

Annex C: Complete table with the data obtained from the enrofloxacin release in buffer A using the Franz Cell

Time	Absorbance			Concentration in the receptor compartment [ug/ml]					Amount of drug released from the hydrogel [ug]				
	Sample 1	Sample 2	Sample 3	Sample 1	Sample 2	Sample 3	Mean	Standard Deviation	Sample 1	Sample 2	Sample 3	Mean	Standard Deviation
0	0,000	0,000	0,000	0,000	0,000	0,000	**0,000**	**0,000**	0,000	0,000	0,000	**0,000**	**0,000**
5	0,323	0,290	0,334	5,778	5,188	5,975	**5,647**	**0,410**	358,247	321,646	370,447	**350,113**	**25,397**
10	0,549	0,448	0,523	9,821	8,014	9,356	**9,064**	**0,938**	608,909	496,887	580,072	**561,956**	**58,166**
15	0,642	0,665	0,685	11,485	11,896	12,254	**11,878**	**0,385**	712,057	737,567	759,750	**736,458**	**23,865**
20	0,841	0,799	0,880	15,045	14,293	15,742	**15,027**	**0,725**	932,773	886,190	976,029	**931,664**	**44,930**
25	1,021	1,055	1,008	18,265	18,873	18,032	**18,390**	**0,434**	1132,415	1170,125	1117,996	**1140,179**	**26,918**
30	1,220	1,280	1,200	21,825	22,898	21,467	**22,063**	**0,745**	1353,131	1419,678	1330,948	**1367,919**	**46,176**
35	1,349	1,338	1,345	24,132	23,936	24,061	**24,043**	**0,100**	1496,208	1484,007	1491,771	**1490,662**	**6,175**
40	1,421	1,458	1,435	25,420	26,082	25,671	**25,725**	**0,334**	1576,064	1617,102	1591,592	**1594,919**	**20,720**
45	1,519	1,550	1,569	27,174	27,728	28,068	**27,657**	**0,452**	1684,758	1719,141	1740,215	**1714,705**	**27,993**
50	1,596	1,610	1,625	28,551	28,801	29,070	**28,807**	**0,259**	1770,161	1785,689	1802,326	**1786,058**	**16,085**
55	1,722	1,701	1,739	30,805	30,429	31,109	**30,781**	**0,341**	1909,911	1886,619	1928,766	**1908,432**	**21,112**
60	1,766	1,761	1,770	31,592	31,503	31,664	**31,586**	**0,081**	1958,712	1953,166	1963,148	**1958,342**	**5,001**
65	1,800	1,810	1,795	32,200	32,379	32,111	**32,230**	**0,137**	1996,422	2007,513	1990,877	**1998,271**	**8,471**
70	1,802	1,800	1,801	32,236	32,200	32,218	**32,218**	**0,018**	1998,640	1996,422	1997,531	**1997,531**	**1,109**
75	1,796	1,804	1,806	32,129	32,272	32,308	**32,236**	**0,095**	1991,986	2000,859	2003,077	**1998,640**	**5,869**
80	1,800	1,800	1,805	32,200	32,200	32,290	**32,230**	**0,052**	1996,422	1996,422	2001,968	**1998,271**	**3,202**

Time (min)	Percentage of drug released from the hydrogel%					Amount of active substance per unit area (Q) [ug/cm2]				
	Sample 1	Sample 2	Sample 3	Mean	Standard Deviation	Sample 1	Sample 2	Sample 3	Mean	Standard Deviation
0	0,00	0,00	0,00	**0,00**	**0,000**	0,000	0,000	0,000	**0,000**	**0,000**
5	17,91	16,08	18,52	**17,51**	**1,270**	37,236	33,432	38,504	**36,391**	**2,640**
10	30,45	24,84	29,00	**28,10**	**2,908**	63,290	51,646	60,292	**58,409**	**6,046**
15	35,60	36,88	37,99	**36,82**	**1,193**	74,011	76,662	78,968	**76,547**	**2,481**
20	46,64	44,31	48,80	**46,58**	**2,246**	96,952	92,110	101,448	**96,836**	**4,670**
25	56,62	58,51	55,90	**57,01**	**1,346**	117,702	121,622	116,204	**118,509**	**2,798**
30	67,66	70,98	66,55	**68,40**	**2,309**	140,643	147,560	138,338	**142,181**	**4,800**
35	74,81	74,20	74,59	**74,53**	**0,309**	155,515	154,247	155,054	**154,938**	**0,642**
40	78,80	80,86	79,58	**79,75**	**1,036**	163,815	168,080	165,429	**165,775**	**2,154**
45	84,24	85,96	87,01	**85,74**	**1,400**	175,113	178,686	180,877	**178,225**	**2,910**
50	88,51	89,28	90,12	**89,30**	**0,804**	183,989	185,603	187,332	**185,642**	**1,672**
55	95,50	94,33	96,44	**95,42**	**1,056**	198,515	196,094	200,475	**198,361**	**2,194**
60	97,94	97,66	98,16	**97,92**	**0,250**	203,587	203,011	204,048	**203,549**	**0,520**
65	99,82	100,38	99,54	**99,91**	**0,424**	207,507	208,660	206,930	**207,699**	**0,880**
70	99,93	99,82	99,88	**99,88**	**0,055**	207,737	207,507	207,622	**207,622**	**0,115**
75	99,60	100,04	100,15	**99,93**	**0,293**	207,046	207,968	208,198	**207,737**	**0,610**
80	99,82	99,82	100,10	**99,91**	**0,160**	207,507	207,507	208,083	**207,699**	**0,333**

Annex D: Complete table with the data obtained for the mathematical models used in the release kinetics.

Time (min)	Percentage of drug released from the hydrogel%					Percentage of drug remaining in the hydrogel %					Log of Cumulative Percentage of Drug Remaining %				
	Sample 1	Sample 2	Sample 3	Mean	SD	Sample 1	Sample 2	Sample 3	Mean	Standard Deviation	Sample 1	Sample 2	Sample 3	Mean	SD
0	0,00	0,00	0,00	**0,00**	**0,00**	100,00	100,00	100,00	**100,00**	**0,00**	2,00	2,00	2,00	**2,00**	**0,00**
5	17,91	16,08	18,52	**17,51**	**1,27**	82,09	83,92	81,48	**82,49**	**1,27**	1,91	1,92	1,91	**1,92**	**0,01**
10	30,45	24,84	29,00	**28,10**	**2,91**	69,55	75,16	71,00	**71,90**	**2,91**	1,84	1,88	1,85	**1,86**	**0,02**
15	35,60	36,88	37,99	**36,82**	**1,19**	64,40	63,12	62,01	**63,18**	**1,19**	1,81	1,80	1,79	**1,80**	**0,01**
20	46,64	44,31	48,80	**46,58**	**2,25**	53,36	55,69	51,20	**53,42**	**2,25**	1,73	1,75	1,71	**1,73**	**0,02**
25	56,62	58,51	55,90	**57,01**	**1,35**	43,38	41,49	44,10	**42,99**	**1,35**	1,64	1,62	1,64	**1,63**	**0,01**
30	67,66	70,98	66,55	**68,40**	**2,31**	32,34	29,02	33,45	**31,60**	**2,31**	1,51	1,46	1,52	**1,50**	**0,03**
35	74,81	74,20	74,59	**74,53**	**0,31**	25,19	25,80	25,41	**25,47**	**0,31**	1,40	1,41	1,41	**1,41**	**0,01**
40	78,80	80,86	79,58	**79,75**	**1,04**	21,20	19,14	20,42	**20,25**	**1,04**	1,33	1,28	1,31	**1,31**	**0,02**
45	84,24	85,96	87,01	**85,74**	**1,40**	15,76	14,04	12,99	**14,26**	**1,40**	1,20	1,15	1,11	**1,15**	**0,04**
50	88,51	89,28	90,12	**89,30**	**0,80**	11,49	10,72	9,88	**10,70**	**0,80**	1,06	1,03	0,99	**1,03**	**0,03**
55	95,50	94,33	96,44	**95,42**	**1,06**	4,50	5,67	3,56	**4,58**	**1,06**	0,65	0,75	0,55	**0,65**	**0,10**
60	97,94	97,66	98,16	**97,92**	**0,25**	2,06	2,34	1,84	**2,08**	**0,25**	0,31	0,37	0,27	**0,32**	**0,05**

Time (min)	Log of Cumulative Percentage of Drug released %					Cube Root of Drug Remaining Percentage %				
	Sample 1	Sample 2	Sample 3	Mean	Standard Deviation	Sample 1	Sample 2	Sample 3	Mean	Standard Deviation
0	0,00	0,00	0,00	**0,00**	**0,00**	4,64	4,64	4,64	**4,64**	**0,00**
5	1,25	1,21	1,27	**1,24**	**0,03**	4,35	4,38	4,34	**4,35**	**0,02**
10	1,48	1,40	1,46	**1,45**	**0,05**	4,11	4,22	4,14	**4,16**	**0,06**
15	1,55	1,57	1,58	**1,57**	**0,01**	4,01	3,98	3,96	**3,98**	**0,03**
20	1,67	1,65	1,69	**1,67**	**0,02**	3,76	3,82	3,71	**3,77**	**0,05**
25	1,75	1,77	1,75	**1,76**	**0,01**	3,51	3,46	3,53	**3,50**	**0,04**
30	1,83	1,85	1,82	**1,83**	**0,01**	3,19	3,07	3,22	**3,16**	**0,08**
35	1,87	1,87	1,87	**1,87**	**0,00**	2,93	2,95	2,94	**2,94**	**0,01**
40	1,90	1,91	1,90	**1,90**	**0,01**	2,77	2,68	2,73	**2,73**	**0,05**
45	1,93	1,93	1,94	**1,93**	**0,01**	2,51	2,41	2,35	**2,42**	**0,08**
50	1,95	1,95	1,95	**1,95**	**0,00**	2,26	2,20	2,15	**2,20**	**0,06**
55	1,98	1,97	1,98	**1,98**	**0,00**	1,65	1,78	1,53	**1,65**	**0,13**
60	1,99	1,99	1,99	**1,99**	**0,00**	1,27	1,33	1,23	**1,28**	**0,05**

Annex E: Release kinetics models

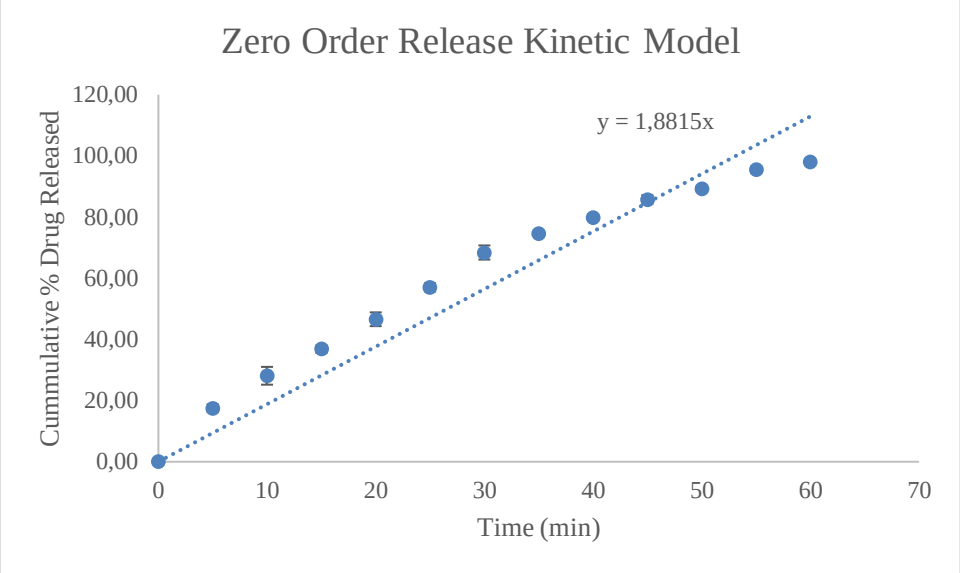

Figure 35: Zero-order release kinetic model

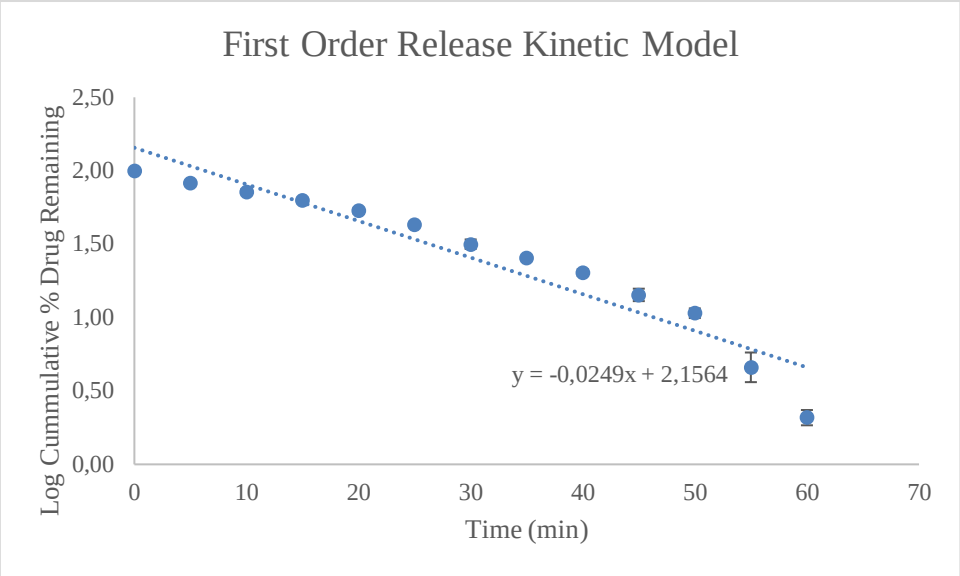

Figure 36: First-order release kinetic model

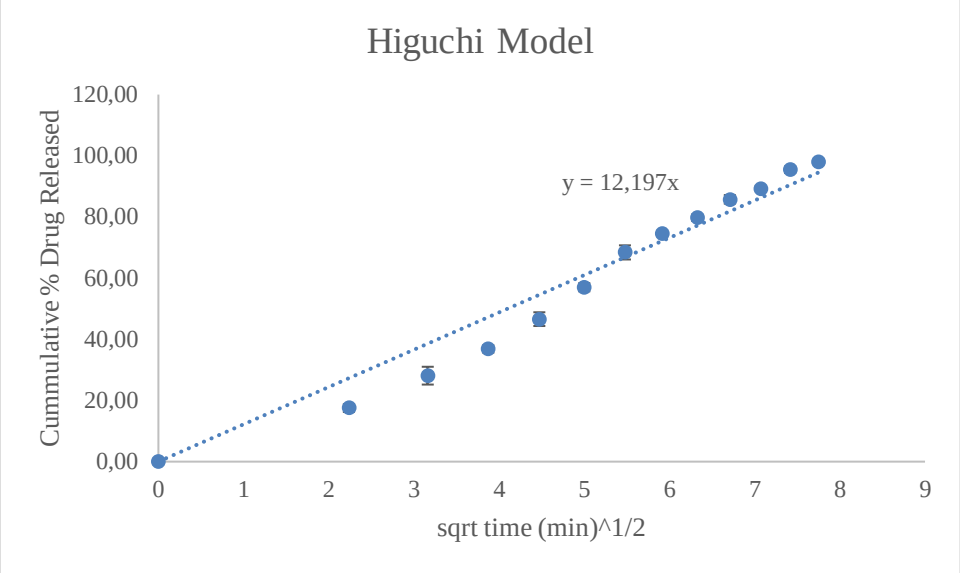

Figure 37: Higuchi model for release kinetics

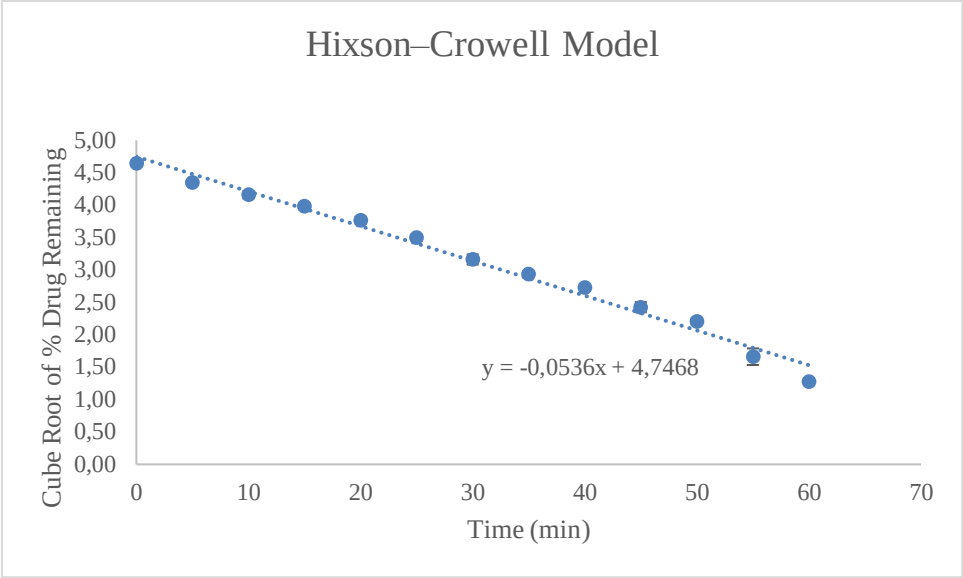

Figure 38: Hixson-Crowell model for release kinetics

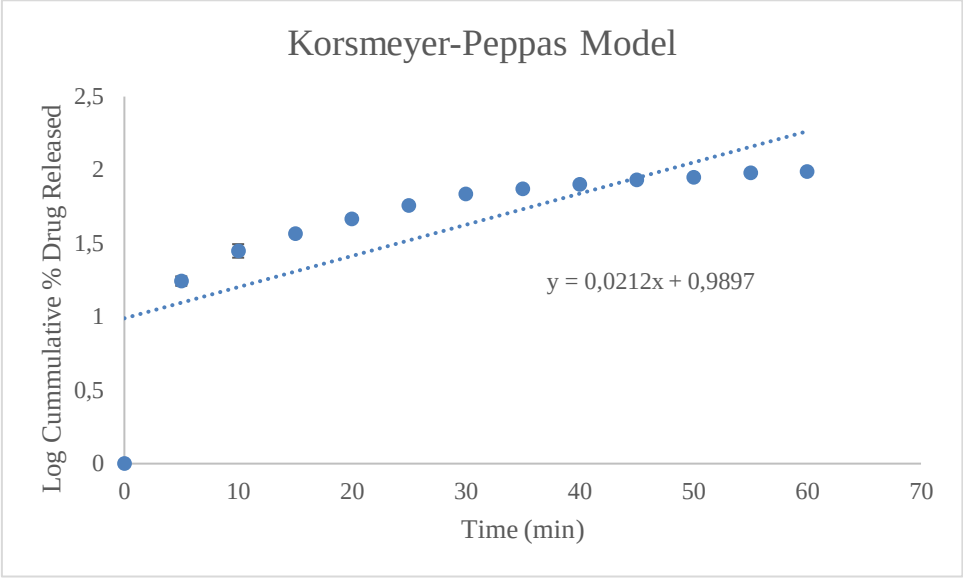

Figure 39: Korsmeyer-Peppas Model for release kinetics